Inductive sensors and directional sensing for PD monitoring in RMUs

Wagenaars, P.

Award date:
2004

TU/e technische universiteit eindhoven

Capaciteitsgroep Elektrische Energietechniek
Electrical Power Systems

Inductive sensors and directional sensing for PD monitoring in RMUs

door: P. Wagenaars
EPS.04.A.173

Afstudeerwerk verricht o.l.v.:

prof. dr. ir. E.F. Steennis
ir. P.C.J.M. van der Wielen
dr. P.A.A.F. Wouters

October 7, 2004

/ faculteit elektrotechniek

Preface

This Master's thesis concludes my graduation project. Completing this project is the final requirement for completing the course Electrical Engineering at the Department of Electrical Engineering at the Eindhoven University of Technology.

The graduation project is part of the larger PD-online project. This project is set up by KEMA and the Electrical Powers Systems group of the Department of Electrical Engineering. I would like to thank prof. dr. ir. E.F. Steennis setting up the PD-online project. Furthermore, I need to thank my direct supervisors ir. P.C.J.M. van der Wielen and dr. P.A.A.F. Wouters for their guidance and support during my graduation project. Finally, I would like to thank Pim Jacobs. He is also a student, working on the PD-online project. He helped me with the measurements on the KEMA test set-up.

Eindhoven, September 2004
Paul Wagenaars

Contents

Summary

For maintenance strategies utilities need to know the current condition of their network. In the past years off-line partial discharge (PD) measurements have proven to provide a lot of useful information on the condition of a cable system. But utilities are reluctant to put a cable off-line. Therefore a new online method is developed to monitor PDs in a cable system. This method requires current sensors in the Ring-Main-Units (RMUs) at both sides of a cable.

Online PD monitoring offers new possibilities. It is possible to monitor a cable system for a longer period of time and monitor several cable systems at the same time. Because it is likely that several cable systems will be monitored simultaneously the price of a test system is important. An important part of a test system are the sensors. Currently, commercial current probes are used. But these are quite expensive. Therefore an alternative is developed in the form of air-core Rogowski coils. This report discusses the feasibility of cheap air-core Rogowski coils for PD monitoring in RMUs. Two coils were designed and built to test the bandwidth, sensitivity and electrical shielding effectiveness.

The sensitivity of both coils is measured with a network analyser and a test set-up. The test set-up is used, to make the influence of the environment constant and the measurements reproducible. The sensitivity of both coils is better than the minimal desired sensitivity, over the major part of the frequency range of interest. Because the coils have resonances in the desired frequency range, it is not possible to use the coils for the entire range. The usable bandwidth is limited by the lowest resonance frequency.

In an RMU, disturbing electric and magnetic fields are present. When a coil is clamped around a conductor, a current can couple capacitively to the coil and cause a disturbing signal at the output. Therefore the coil must be shielded for electrical fields. A test set-up with an electrode through the large loop of the coil was developed. With this test set-up two different coils are tested for their shielding effectiveness. The shielding of the coil made with coaxial cable is about 2-3 times as effective as a coil made with copper wire. The screen of the coaxial cable is interrupted after every turn. All screen sections are connected to each other by a common earth wire around the coil. At the end of the coil the screen and conductor are short-circuited.

In an RMU, the cable under test is not the only possible source of PDs. When the direction of each measured pulse is determined, it is known whether the pulse comes from the cable under test or not. Two methods to determine the pulse direction are developed. The first method is called the Polarity-of-First-Peak (PFP) method. On two locations in the RMU the current is

measured. The combination of the polarities of the first peak of both currents gives the direction of the pulse. Measurements showed that this method works very good. The main disadvantage of this method is the requirement that the pulses can be clearly separated from each other.

A second directional sensing method was developed. For this method the pulses do not need to be separated as clearly. This sensing method also measures the current at two locations in the RMU. These two currents are combined into one signal. The resulting signal only contains the incoming pulses from the cable under test. Disturbing outgoing pulses are removed from the resulting signal. Measurements on a test set-up showed that the method works reasonably well. Pulses from the cable under test remain unchanged while disturbing pulses coming from another 10kV cable are removed from the signal. Disturbing pulses from the transformer are not removed from the signal. They can cause a disturbing signal with about the same amplitude as the original pulse.

List of Symbols

For an explanation of the current symbols: i_1, i_2, i_{tcce}, i_{plec}, i_{tcc}, i_{3tcc}, i_{lec} and i_{tr} and the impedance symbols: Z_1, Z_2, Z_{tcce}, Z_{plec}, Z_{3tcc} and Z_{tr}, see appendix A on page 53.

A	cross section of a coil turn (m^2)
C_{ec}	capacitance on shielding test board between electrode and coil (F)
C_{par}	capacitance on the shielding test board in parallel with L_{loop} and C_{ec} (F)
C_{sw}	capacitance between screen and winding of a shielded Rogowski coil (F)
c	capacitance C_{sw} per unit length (=C_{sw}/G) (F/m)
f_{co}	cut-off frequency (Hz)
G	length of the coil (m)
$H_{tcce,1}$	transfer function from I_{tcce} to I_1 (-)
$H_{tcce,1,in}$	transfer function I_1/I_{tcce} for incoming pulses (-)
$H_{tcce,1,out}$	transfer function I_1/I_{tcce} for outgoing pulses (-)
h	Rogowski coil height (m)
i_{enc}	current enclosed by a loop or Rogowski coil (A)
I_{inj}	current injected capacitively into the coil with the shielding test set-up (A)
I_{pr}	primary current (A)
i_{sec}	secondary current, current through coil turns (A)
L	self inductance of a Rogowski coil (H)
L_{loop}	inductance of the loop of the shielding test board (H)
l	self inductance per unit length (=L/G) (H/m)
M	mutual inductance (H)
m	mutual inductance per unit length (=M/G) (H/m)
N	number of turns (-)
n	turn density (turns/m)
r_1	inner Rogowski coil radius (m)
r_2	outer Rogowski coil radius (m)
v_{pr}	primary voltage, between environment and coil (V)
v_{sec}	secondary voltage at terminals (V)
v_{ind}	induced voltage at secondary of a Rogowski coil side (V) (= $j\omega M I_1$)

Lists continues on next page

Z_{ec}	impedance between electrode of the electrical shielding test set-up and the coil under test (Ω)
Z_i	input impedance as seen from the network analyser (Ω)
Z_L	load impedance (Ω)
Z_{secinj}	transfer impedance from I_{inj} to V_{sec} (Ω)
Z_t	transfer impedance (Ω) ($= V_{sec}/I_{pr}$)
ϕ_{enc}	magnetic flux enclosed by one winding (Wb)
ϕ_{tot}	magnetic flux enclosed by all windings (Wb)
ω_{co}	cut-off angular velocity (rad/s)

Chapter 1

Introduction

In the Netherlands alone there is about 90,000 km medium voltage power cable installed for the distribution of electrical power. A large part of these cables is relatively old and utilities want to know when they need to be replaced. Unfortunately, it is complicated to determine the exact remaining life of these cables. In such a situation the maintenance strategy of the cable systems is very important.

Utilities are shifting their focus from events based maintenance (EBM) to condition based maintenance (CBM). With EBM, action is taken after a failure has taken place. With CBM on the contrary, action is taking place before failure. A network owner in the U.S.A. calculated that condition based maintenance saves money, each dollar spent on diagnostic measurements saves about 1.5 dollar for a typical mixed network [Ste04]. As the name suggests, for CBM the current condition of the network has to be known.

There are several diagnostic methods to determine the condition of cable systems. One of the diagnostic methods available for medium voltage cables are partial discharge (PD) measurements. Monitoring the PDs in a cable system gives a lot of information on the current state of the cable. At the moment a cable has to be taken out of service before the cable can be tested. Utilities are reluctant to put a cable off-line and in some situations a cable can not be taken off-line without interrupting the power delivery to some customers. Therefore an online method to measure PDs in medium voltage (MV) cables is being developed.

One of the most important parts in a measurement system are the sensors. In an online measurement system the sensor must be installed without interrupting the power delivery and without compromising safety standards. One option is to use commercially available general purpose current probes with a ferromagnetic core. But these sensors can be quite expensive. If it would be possible to replace the commercial sensors with cheap air core Rogowski coils [Rog12], the sensor costs will be reduced significantly, making it cheaper to monitor several cable systems simultaneously. Air core Rogowski coils are less sensitive than sensors with a ferromagnetic core. This is not by definition a problem, if also susceptibility for interference is reduced. Moreover, if air core Rogowski coils are optimised for their specific application, it is likely that they can replace expensive sensors with ferromagnetic core. This report discusses the design of such a sensor.

The sensors will be installed in the Ring Main Units (RMUs) at the beginning and end of the MV cable under test. Because most RMUs consist of more than one incoming cable there are

several sources from which a measured PD can originate. For cable testing, only the PDs originating from the cable under test should be recorded. If the sensors are directional sensitive, the direction of PD pulses is known and thus also the origin of the PD pulses. Including directional sensitivity to the sensors is a second subject in this report.

The structure of this report is as follows:

Chapter 2 Discusses the general theory of a Rogowski coil.

Chapter 3 Describes the design considerations of several aspects of the designed coils.

Chapter 4 Describes measurements of the transfer impedance of the realised coils.

Chapter 5 Describes a test set-up to measure the electrical shielding effectiveness of coils and presents the experimental results for two coils.

Chapter 6 Discusses two developed directional sensing techniques that can be used online in an RMU.

Chapter 7 Summarises the conclusions and gives recommendations for future research.

Chapter 2

Rogowski coil theory

A Rogowski coil has a core (air) with a toroidal shape. The coil is placed around a conductor. A current through the conductor produces a magnetic field inducing a voltage over the coil. This voltage is proportional to the rate of change of the current through the conductor. The Rogowski coil was first described by W. Rogowski and W. Steinhaus in 1912 [Rog12].

2.1 Mutual inductance

A primary current through the large loop of the Rogowski coil induces a voltage in the secondary winding of the coil. This voltage v_{ind} is proportional to the rate of change of the primary current i_{pr} with a factor M. This factor is the mutual inductance.

$$v_{ind} = M\frac{di_{pr}}{dt} \quad \text{or} \quad V_{ind} = j\omega M I_{pr} \tag{2.1}$$

The value of the mutual inductance is calculated for different coil configurations in the following sections.

2.1.1 Thin Rogowski coil

The Rogowski coil can be seen as an illustrative application of Ampère's law [War93]. This law provides the relation between a current and the magnetic field in a closed loop around it. This relation is given by:

$$\oint \vec{H} \cdot \vec{dl} = i_{enc} \quad \text{or} \quad \oint H\cos(\alpha)dl = i_{enc} \tag{2.2}$$

where dl is a small length along the loop, H is the magnetic field, α is the angle between the magnetic field H and an element dl and i_{enc} is the current enclosed by the loop. When the next assumptions are made this law can be used to derive the Rogowski coil response.

- The cross section of the turns is small compared to the coil diameter, so the magnetic field H can be considered constant over the turn cross section.
- The winding density n is high and constant.

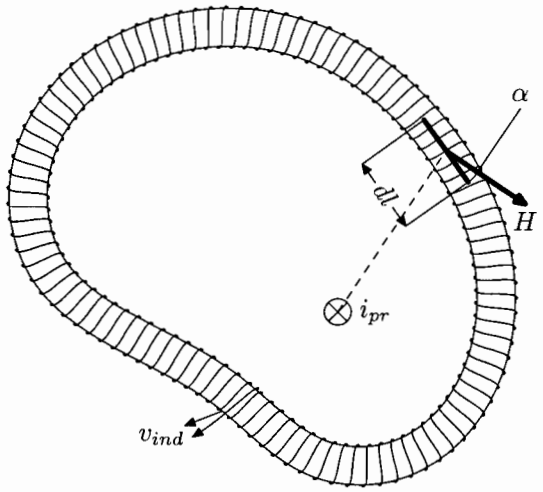

Figure 2.1: Long, thin helical coil

Consider a long, thin helical coil enclosing a current, as in figure 2.1. The current i_{pr} produces a magnetic field H. The coil has n turns per metre and a cross section A. A section dl has ndl turns. The magnetic flux linkage in one dl section is

$$d\phi = \mu H A n dl \cos(\alpha) \tag{2.3}$$

Where μ is the magnetic permeability. The total flux enclosed by the entire coil (ϕ_{tot}) is given by integrating $d\phi$ along the coil:

$$\phi_{tot} = \int d\phi = \mu n A \int H \cos(\alpha) dl = \mu n A i_{pr} \tag{2.4}$$

In the last step Ampère's law (equation 2.2) is used to evaluate the integral. The voltage at the terminals is given by the rate of change of the enclosed flux:

$$v_{ind} = \frac{d\phi_{tot}}{dt} = \mu n A \frac{di_{pr}}{dt} \tag{2.5}$$

A Rogowski coil is often expressed in terms of a mutual inductance M between the coil and the conductor (equation 2.1). The mutual inductance M in equation 2.5 is given by: $M = \mu n A$.

2.1.2 Coil with larger cross section

When the coil area is larger, the assumption that the magnetic field H is constant over the entire cross section is no longer valid. It that case the method to calculate the mutual inductance M (section 2.1.1) can not be used anymore. But also for a larger cross section the coil can be modelled as a mutual inductance. For a coil with rectangular cross section and a current through the centre of the coil (figure 2.2) the mutual inductance can be calculated as follows. Again Ampère's law is used as a starting point. Consider a circle with a radius r and a current i_{pr} through the middle.

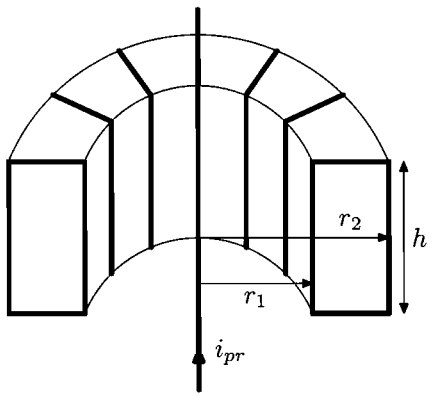

Figure 2.2: Rogowski coil with rectangular cross section

Then the amplitude of the magnetic field H is constant along the circle. The magnetic flux density B on the circle can be calculated using Ampère's law (equation 2.2):

$$2\pi r H = i_{pr} \quad \Rightarrow \quad B = \frac{i_{pr}\mu}{2\pi r}$$

The magnetic flux enclosed by one turn ϕ_{enc} is calculated by integrating B over the cross section:

$$\phi_{enc} = \int_0^h \int_{r_1}^{r_2} \frac{i_{pr}\mu}{2\pi r} dr dz = h\frac{i_{pr}\mu}{2\pi} \ln\left(\frac{r_2}{r_1}\right) \tag{2.6}$$

This flux is enclosed by every single turn. So the total enclosed flux ϕ_{tot} is:

$$\phi_{tot} = N \cdot \phi_{enc} = Nh\frac{i_{pr}\mu}{2\pi} \ln\left(\frac{r_2}{r_1}\right) \tag{2.7}$$

Where $N = n \cdot G$ the total number of turns and G the length of the coil. The voltage induced in the coil is:

$$v_{ind} = \frac{d\phi}{dt} = \frac{Nh\mu}{2\pi} \ln\left(\frac{r_2}{r_1}\right) \frac{di_{pr}}{dt} \tag{2.8}$$

So the mutual inductance M is given by:

$$M = \frac{Nh\mu}{2\pi} \ln\left(\frac{r_2}{r_1}\right) \tag{2.9}$$

2.2 Self inductance

A current flowing through the winding causes a magnetic flux opposing the flux caused by the primary current. Therefore the enclosed flux and thus the induced voltage is less than without a current through the coil winding. This means that when the coil is terminated with a finite impedance the output voltage will be smaller than when left completely open. This effect can be modelled with a self inductance. A current flowing through the winding causes a voltage drop across the self inductance and thus a lower voltage at the output terminals.

In the following sections the self inductance is calculated for the same coil configurations as used for the calculation of the mutual inductance in section 2.1.

2.2.1 Thin Rogowski coil

The calculation of the self inductance is similar to the calculation of the mutual inductance. The flux linkage in a dl section is obtained from equation 2.3. The equation for the total flux is the same as equation 2.4, except for the enclosed current, which is now $N \cdot i_{sec}$. The current through a winding i_{sec} is enclosed N times. So the total enclosed flux is the same as equation 2.4 with i_{pr} substituted with $N \cdot i_{sec}$.

$$\phi_{tot} = \int d\phi = \mu n A \int H \cos(\alpha) dl = \mu n A N i_{sec} \tag{2.10}$$

The self inductance L is given by:

$$L = \frac{\phi_{tot}}{i_{sec}} = \mu n A N \tag{2.11}$$

2.2.2 Coil with larger cross section

Again, instead of enclosing the current i_{pr} once, now the coil current i_{sec} is enclosed N times. Consider a four turn coil as depicted in figure 2.3. The four turns carry a current i_{sec}. For a

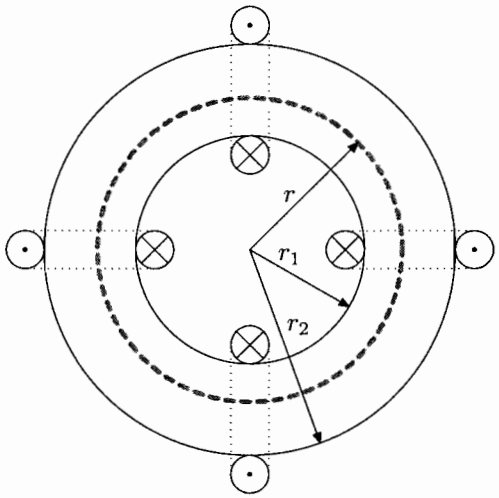

Figure 2.3: Rogowski coil with four turns

concentric circle with a radius r between r_1 and r_2, the magnetic field is given by (derived from equation 2.2):

$$H = \frac{i_{enc}}{2\pi r} = \frac{N \cdot i_{sec}}{2\pi r} \tag{2.12}$$

The magnetic flux enclosed by one rectangular turn is given by:

$$\phi_{enc} = \iint \vec{B} \cdot d\vec{A} = \int_{r_1}^{r_2} \int_0^h \frac{\mu N i_{sec}}{2\pi r} = \frac{h \mu N i_{sec}}{2\pi} \ln\left(\frac{r_2}{r_1}\right) \tag{2.13}$$

The self inductance L is given by the total enclosed flux divided by the current.

$$L = \frac{\phi_{tot}}{i_{sec}} = \frac{N \cdot \phi_{enc}}{i_{sec}} = \frac{N^2 h \mu}{2\pi} \ln\left(\frac{r_2}{r_1}\right) \tag{2.14}$$

2.3 Equivalent circuits

2.3.1 Plain equivalent circuit

The first equivalent circuit consists of a current controlled voltage source representing the voltage induced by i_{pr} (see equation 2.1). An inductance L representing the self inductance of the coil and an impedance Z_L representing the load of the Rogowski coil (i.e. a 50Ω coaxial cable to an oscilloscope). The circuit is depicted in figure 2.4.

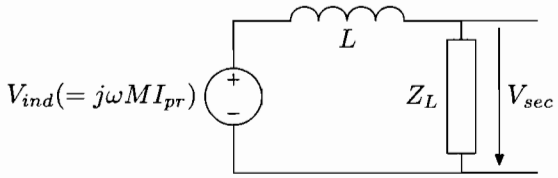

Figure 2.4: Equivalent circuit

The transfer impedance Z_t is given by:

$$Z_t = \frac{V_{sec}}{I_{pr}} = \frac{j\omega M Z_L}{Z_L + j\omega L} \tag{2.15}$$

For an infinite load impedance Z_L the output voltage v_{sec} is equal to the induced voltage v_{ind}. But when the impedance is finite, a small current will flow through the winding causing a voltage drop over the self inductance L. For low frequencies this voltage drop can be neglected. Then v_{sec} is equal to v_{ind} and thus proportional to di_{pr}/dt. For high frequencies this voltage drop can not be neglected anymore, since the impedance of L becomes much larger than Z_L. Both the induced voltage and the impedance of the self inductance are proportional to the frequency. The extra voltage that is induced for higher frequencies falls entirely across the self inductance. This means that the voltage across Z_L is proportional to i_{pr} and no longer to the time derivative of i_{pr}. This mode of operation is often called the self-integrating mode of a Rogowski coil or such a coil is called a current transformer. The cut-off frequency between differentiating and self integrating mode can be derived from equation 2.15.

$$\omega L = Z_L \quad \Rightarrow \quad \omega_{co} = \frac{Z_L}{L} \text{ or } f_{co} = \frac{Z_L}{2\pi L} \tag{2.16}$$

Where ω_{co} is the cut-off frequency in rad/s and f_{co} the cut-off frequency in Hz. For frequencies well below and above the cut-off frequency the equation for the transfer impedance can be simplified:

$$\begin{aligned} Z_t &= j\omega M \quad \text{for } \omega \ll \omega_{co} \\ Z_t &= \frac{M Z_L}{L} \quad \text{for } \omega \gg \omega_{co} \end{aligned} \tag{2.17}$$

2.3.2 Inter-turn capacitance

There is a small capacitance between the turns of the winding. Consider a single turn of the entire coil. The turn represents a small inductance l and a small capacitance c to the next turn. This capacitance is in parallel with the inductance. The entire coil has N of these sections in series. This series of LC-combinations can be combined into one LC-combination with $L = l \cdot N$ and $C = \frac{c}{N}$. The equivalent circuit is drawn in figure 2.5.

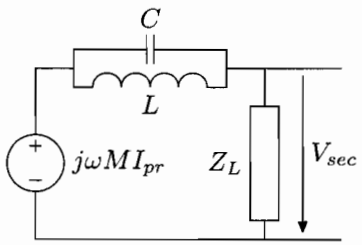

Figure 2.5: Equivalent circuit with inter-turn capacitance

The transfer impedance for this model is given by:

$$Z_t = \frac{V_{sec}}{I_{pr}} = j\omega M \cdot \frac{1}{1 + \frac{j\omega L/Z_L}{1-\omega^2 LC}} \tag{2.18}$$

This transfer impedance has a sharp dip at the resonance frequency of the LC-combination. The voltage v_{sec} is equal to zero at the notch frequency ($1/\sqrt{LC}$) because the impedance of the parallel LC is infinite and the induced voltage falls entirely across it.

2.3.3 Transmission line effects

A Rogowski coil is often used in an environment with disturbing electric fields. These disturbances can be suppressed by a conducting screen around the coil (see section 3.5, [Bos00], [Bel85] and [Coo63]). This screen can also be used as a return winding. That is achieved with a short-circuit between the coil winding and screen at one side and a termination with an impedance at the other side (e.g. 50Ω coaxial cable to the oscilloscope). The equivalent circuit of a small section is drawn in figure 2.6. The induced voltage due to the primary current and mutual inductance is represented by a voltage source, the self inductance by an inductance and the capacitance between winding and screen by a capacitance. The symbols l, m and c are respectively the self inductance, mutual inductance and capacitance per unit length.

Using the equivalent circuit the following transmission line equations can be written:

$$\frac{dV(x,\omega)}{dx} = -j\omega l I(x,\omega) + j\omega m I_{pr}(\omega) \tag{2.19}$$

$$\frac{dI(x,\omega)}{dx} = -j\omega c V(x,\omega) \tag{2.20}$$

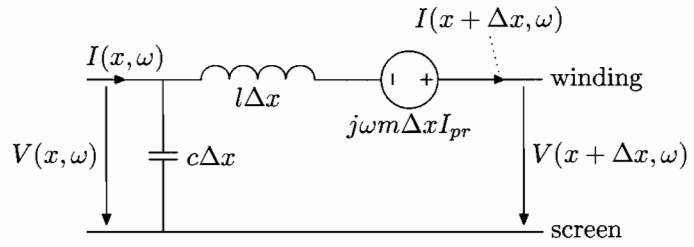

Figure 2.6: Equivalent circuit transmission line section

Where $l = L/G$ (self inductance per unit length), $m = M/G$ (mutual inductance per unit length) and $c = C_{sw}/G$ (capacitance per unit length) with C_{sw} the capacitance between screen and winding.

These equations are typical transmission line equations. They can be solved using the boundary conditions. The coil is short circuited at $x = 0$ and terminated with impedance Z_L at $x = G$.

$$V(x = 0, \omega = 0) = 0 \quad \text{and} \quad \frac{V(x = G, \omega)}{I(x = G, \omega)} = Z_L$$

The output voltage at $x = G$ is given by the equation below (see [Bos00]).

$$V_{sec} = V(G, \omega) = \frac{Z_L \frac{m}{l} I_{pr} \sinh(\gamma(\omega)G)}{\frac{Z_L}{Z_0} \cosh(\gamma(\omega)G) + \sinh(\gamma(\omega)G)} \tag{2.21}$$

With $Z_0 = \sqrt{\frac{l}{c}}$ the characteristic impedance of the coil and $\gamma(\omega) = j\omega\sqrt{lc}$.

The output of an transmission line becomes zero when the length of the coil is an integer multiple of half the wavelength. Then a standing wave occurs in the transmission line. This can also be explained using the condition that equation 2.21 is equal to zero, when the numerator is equal to zero.

$$\begin{aligned} Z_L \tfrac{m}{l} I_{pr} \sinh(\gamma(\omega)G) &= 0 \\ \gamma(\omega)G &= jk\pi \\ j2\pi f\sqrt{lc}G &= jk\pi \\ 2f\sqrt{LC_{sw}} &= k \\ f_{notch}(k) &= \tfrac{k}{2\sqrt{LC_{sw}}} \end{aligned} \tag{2.22}$$

Where k is a positive integer.

Equation 2.21 can be simplified for low frequencies. The following simplifications are made:

$$|\gamma(\omega)G| \ll 1 \;\Rightarrow\; \cosh(\gamma(\omega)G) \approx 1 \text{ and } \sinh(\gamma(\omega)G) \approx \gamma(\omega)G$$

Substituting these equations in equation 2.21 yields:

$$V(G, \omega) = \frac{Z_L \frac{m}{l} I_{pr} \gamma(\omega)G}{\frac{Z_L}{Z_0} + \gamma(\omega)G} = \frac{Z_L \cdot I_{pr} \cdot mG \cdot j\omega\sqrt{\frac{c}{l}}}{Z_L\sqrt{\frac{c}{l}} + j\omega\sqrt{lc}G} = I_{pr}\frac{j\omega M Z_L}{Z_L + j\omega L} \tag{2.23}$$

Equation 2.21 shows that for frequencies well below the lowest notch frequency the transfer impedance is the same as the transfer impedance for the plain equivalent circuit (equation 2.15).

Chapter 3

Coil design

3.1 Design criteria

The Rogowski coil to be designed is restricted by several criteria.

- inner radius: $r_1 > 33.5$ mm
  To make sure that the coil fits around most MV cables.

- outer radius: $r_2 < 60.5$ mm
  The space around the cable is limited.

- height: $h < 60$ mm
  The space where the coil can be installed is limited.

- bandwidth: 30 kHz – 30 MHz
  PDs are phenomena with a large frequency range. However higher frequencies attenuate stronger than lower frequencies. Therefore high frequencies travel less far than lower frequencies. Looking at frequencies higher than tens of MHz is useless because only PDs originating from the first part of the cable (close to the sensor) can then be detected. Higher frequencies from PDs further away are attenuated completely.
  For PD monitoring also the location of the PD source (within the cable) must be determined. With lower frequencies it is not possible to determine the location with high precision. Therefore it is not useful to measure below 30 kHz.

- good suppression of the main power frequency (50 Hz)
  The amplitude of main power frequency is large. To prevent clipping of the digitiser or oscilloscope, it must be attenuated sufficiently.

- sensitivity: 1 V/A
  The commercial sensors that are currently used have a sensitivity of 1 V/A over the entire frequency range. To be competitive in measuring small PD currents, a sensitivity in this order of magnitude is required.

- insensitive to disturbing electric and magnetic fields
  In an RMU disturbing electric and magnetic fields are present. For good measurements these fields may not cause a signal on the output of the sensor.

3.2 Dimensions

The geometry is the most important factor for the performance of the Rogowski coil. The dimensions are restricted by the environment. The inner diameter is determined by the diameter of the thickest cable it has to be clamped around. The maximum height and outer diameter are limited by the space available around the conductor.

For maximum sensitivity the transfer impedance has to be maximised. Equation 2.15 shows the transfer impedance for a plain equivalent circuit. For frequencies well below the cut-off frequency the term $j\omega L$ in the denominator can be neglected (see equation 2.17). This shows that the mutual inductance M needs to be maximised. This is done by making the cross section as large as possible. For a rectangular cross section this means a maximum h and r_2 and minimum r_1.

For frequencies above the cut-off frequency the term Z_L in the denominator can be neglected (see equation 2.17). Because M is in the numerator and L in the denominator and both are proportional to the cross section, the cross section is irrelevant for Z_t for high frequencies.

3.3 Number of turns

Another parameter that can be varied to optimise Z_t is the number of turns. The mutual inductance M is proportional to N, while the self-inductance L is proportional to N^2. Therefore the transfer impedance is proportional to:

$$Z_t = j\omega M \propto N \quad \text{for } \omega \ll \omega_{co} \tag{3.1}$$

$$Z_t = \frac{MZ_L}{L} \propto \frac{N}{N^2} = \frac{1}{N} \quad \text{for } \omega \gg \omega_{co} \tag{3.2}$$

This means that for low frequencies a high number of turns is best and for high frequencies a low number of turns is best. A larger number of turns causes a larger self induction and thus a lower cut-off frequency (see equation 2.16). That means that there is an optimal number of turns as a trade off between these two. It must be noted that ω_{co} is strongly influenced by the number of turns. Anyhow, a large M/L ratio favours single turn Rogowski coils, and high M should be realised through size. Since this results in sizes larger that the dimension criteria allow, the number of turns has to be chosen larger. In fact, it is chosen such that the minimal required ω_{co} is obtained. A detailed analysis of the optimal number of turns [Vae04] showed that close to 10 turns is optimal in case of the desired dimension and frequency range.

3.4 Load impedance

The load impedance Z_L has also an influence on the transfer impedance, since the cut-off frequency is directly proportional to Z_L (equation 2.16). For frequencies below the cut-off frequency,

Z_L has no influence on Z_t (equation 2.17), while for frequencies above the cut-off frequency Z_t is directly proportional to Z_L.

From a practical point of view it would be best to terminate the coil with a standard 50 Ω coaxial cable. A lower load impedance can be achieved with a resistor in parallel with the coaxial cable. Increasing the impedance, on the other hand, is not that easy. A higher load impedance can be achieved by terminating the coil with the desired higher load impedance, in parallel with a buffer or amplifier with an input impedance much higher than Z_L. From an EMC point of view this is not desired since the power leads to the buffer/amplifier will pick up EM interference.

The Z_t averaged over the entire bandwidth is maximal when $f_{oc} > 30$ MHz. Making Z_L larger than that has no influence on Z_t over the desired bandwidth. The theoretical self inductance calculated with equation 2.14 and $h = 6$ mm, $N = 8$, $r_1 = 34$ mm and $r_2 = 64$ mm gives $L = 486$ nH. If the cut-off frequency must be 30 MHz, the Z_L can be calculated with equation 2.16. In that case Z_L must be 92 Ω or higher.

3.5 Electrical shielding

Electric fields couple capacitively to the turns of the coil. The effects of signals that couple in capacitively can be minimised with an conducting screen around the coil. The disturbing signals then couple to the screen. If the screen is properly connected to earth the current will flow to earth without causing a voltage at the output.

The first option is to place a conducting screen around the coil (see [Bel85], [Bos00], [Coo63]). In most situations the screen and winding are short circuited at one end. Another option is to use coaxial cable for the winding [Ger02]. In this paper a coil is described with a coaxial cable. Every turn the screen is interrupted. The primary current also induces a voltage in the earth screen. When the screen is never interrupted the induced voltage causes a current through the screen. This current produces a magnetic flux that opposes the flux of the primary current and virtually no flux remains to induce a voltage in the conductor of the coil. The interruptions divide the screen into separate sections. All sections are connected to each other by a common wire running around the coil. Because of this earth wire all capacitances between the screen of one turn to the screen of the next turn is short-circuited. This prevents resonances caused by these capacitances in combination with the self inductance. At the end the conductor and screen are short circuited. (see figure 3.1).

3.6 Realised coils

Two coils are built and tested. In this section both coils are described. In the next chapters (chapter 4 and chapter 5) the sensitivity (or transfer impedance) and shielding effectiveness of these coils are discussed.

Figure 3.2 shows pictures of both realised coils. Both coils have the same dimensions, the same number of turns and the same load impedance. The difference between both coils is that the winding of the first coil (Rog1) is made of normal copper wire and the winding of the second coil (Rog2) is made of coaxial cable (RG 58C/U). Because the coaxial cable is not as flexible as the copper wire, the coaxial cable turns are slightly round. Therefore the inner diameter is slightly

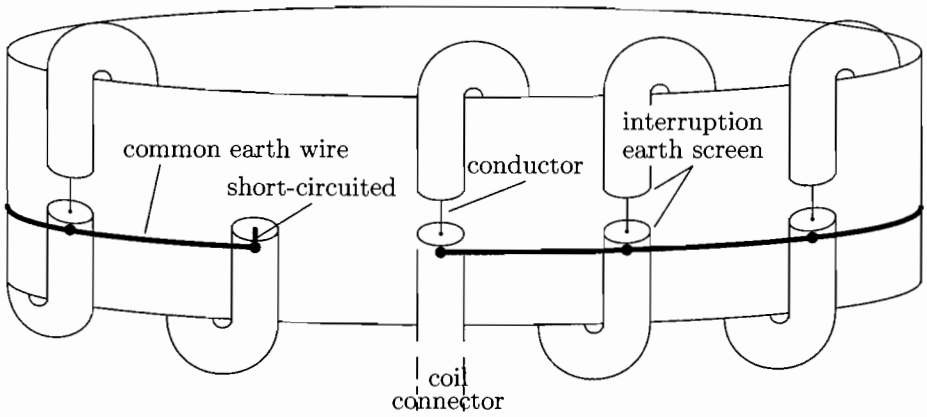

Figure 3.1: Rogowski coil with coaxial cable with interruptions in the earth shield

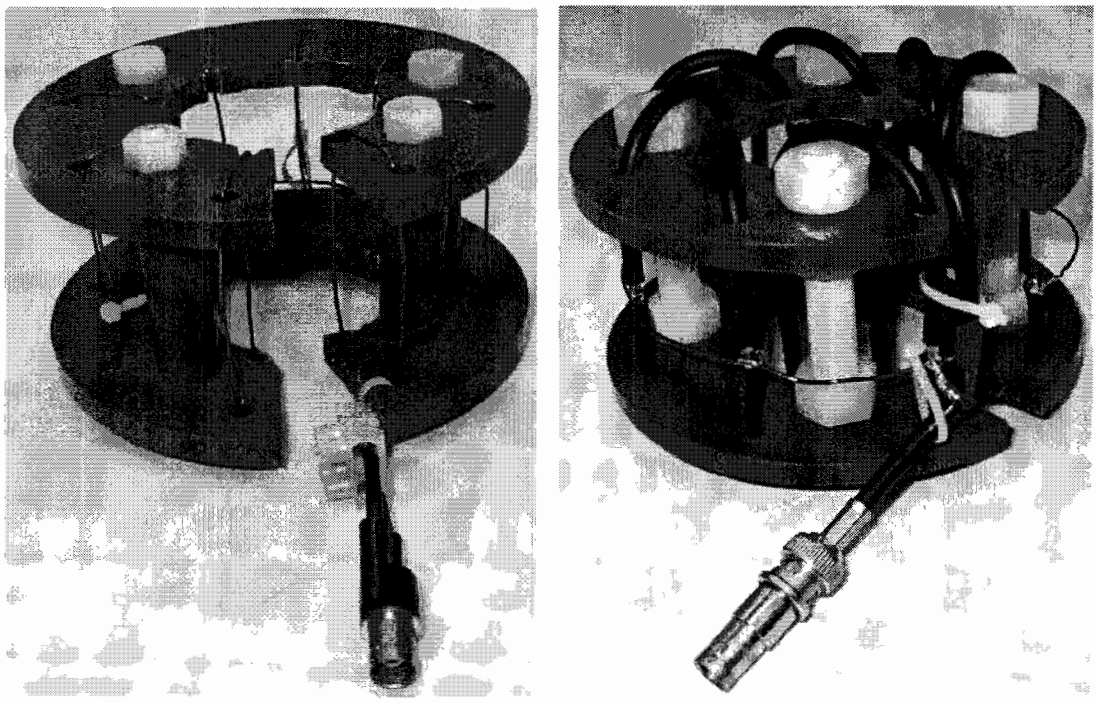

(a) Rogowski coil 1 (Rog1)

(b) Rogowski coil 2 (Rog2)

Figure 3.2: Realised Rogowski coils

less and the turns are slightly higher. The coaxial cable is configured as described in section 3.5 and figure 3.1. The dimensions are:

- inner radius: $r_1 = 30$ mm
- outer radius: $r_2 = 55$ mm
- height: $h = 62$ mm
- number of turns: $N = 8$

Chapter 4

Transfer impedance

4.1 Theoretical transfer impedance

The theoretical sensitivity or transfer impedance of Rog1 (copper wire) can be described by the equivalent circuit in section 2.3.1. Because the distance between the turns is quite large, it is expected that the inter-turn capacitance (as described in section 2.3.2) can be neglected.

Because Rog2 (coaxial cable) has an earth screen, it is expected that the transfer impedance from section 2.3.3 is applicable for this coil. Depending on the values for the mutual inductance, self inductance, capacitance and load impedance, this transfer impedance can be simplified for low frequencies (wavelength much shorter than the length of the coil). This is explained in more detail in section 2.3.3. In that case the transfer impedance is the same as for Rog1.

Because the dimensions of both coils are similar for both coils, the mutual inductance and self inductance will be similar. The mutual inductance is calculated with equation 2.9: $M = 60$ nH . The self inductance is calculated with equation 2.14: $L = 480$ nH . The self inductance is be larger because the wire itself has an inductance and because the coil has a low number of turns, a lot of flux is present around the turns, contributing to the self inductance and not to the mutual inductance. Both coils are loaded with a characteristically terminated 50Ω coaxial cable.

For the transmission line model, the quantities m, l, c and G are required. The average radius of Rog2 is about 42 mm, thus the length of the coil is $G = 26$ cm. That means that $m = M/G = 230$ nH/m and $l = L/G = 1.8$ μH/m. The capacitance of an RG58 coaxial cable is about 100 pF/m. One turn has 0.174 m coaxial cable, so the total capacitance of 8 turns is: 139 pF. The capacitance per unit length of the coil: $c = 139/0.26 = 535$ pF/m. The lowest notch frequency is calculated with equation 2.22: $f_{notch}(1) = 62$ MHz.

4.2 Transfer impedance test set-up

When the transfer impedance of a coil is measured, the environment may have an influence. To make the influence constant and the measurements reproducible, a test set-up is constructed. The test set-up is drawn schematically in figure 4.1. In the test set-up, the coil is enclosed at four sides by a conducting brass screen. The coil is clamped around the conductor in the middle. The current through this conductor is the primary current I_{pr}. At the left and right hand side of the

test set-up, N-type connectors are installed. The shields of these connectors are connected to the brass screen of the test set-up. The conductors of these connectors are connected to both sides of the primary conductor in the middle of the test set-up. The connector at one side of the test set-up is connected to port 1 of a network analyser and the connector at the other side is terminated with 50 Ω. This terminating impedance could be any impedance, as long as it is not so large that the primary current becomes too small to be detected by the coil. The brass enclosing is the return path. The coil connector is connected with port 2 of the test set-up.

With the network analyser, the S-parameters S_{11} and S_{21} are measured. S-parameters are the reflection and transmission coefficients between incident and reflection waves for a network with 1 or more ports. S_{11} is the ratio of the reflected wave to the incident wave on port 1. S_{21} is the ratio of the output of port 2 to the incident wave on port 1. These S-parameters can be converted into the transfer impedance $Z_t = V_{sec}/I_{pr}$.

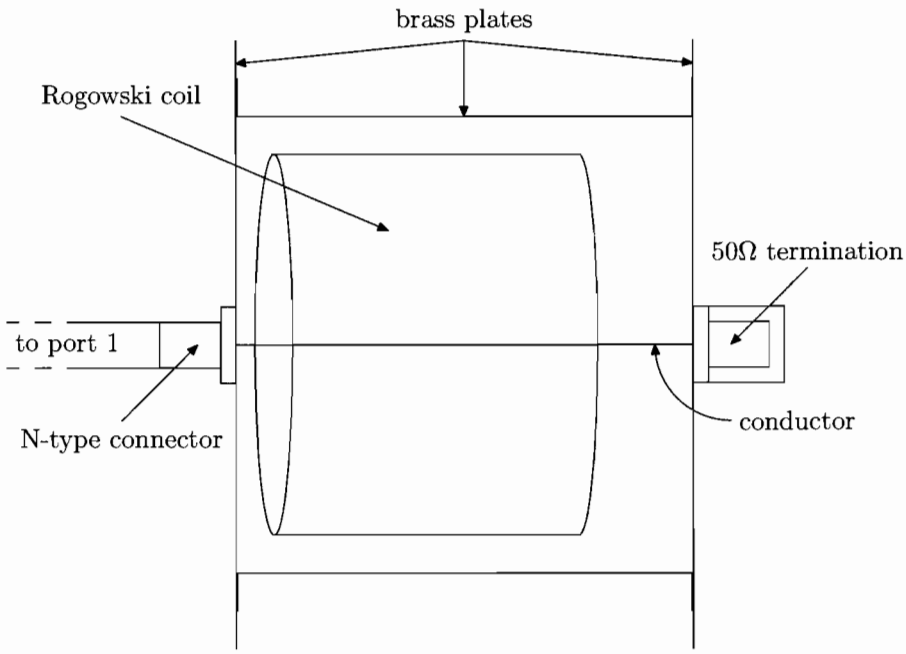

Figure 4.1: Test set-up for transfer impedance measurements

4.3 Measurement results

The transfer impedance (or sensitivity) of both coils is measured with the test set-up described in section 4.2.

- In figure 4.2 the measured transfer impedance of Rog1 is plotted. Both the measured and a calculated transfer impedance are plotted. The values for M and L are fitted to make the calculated transfer impedance match the measured transfer impedance as good as possible: $M = 60$ nH and $L = 1.4$ μH.

- In figure 4.3 the measured transfer impedance of Rog2 is plotted together with the calculated transfer impedance. Note that frequency axis for this graph goes up to 100 MHz, instead of 50 MHz. The values for m, l and c are fitted to make the calculated transfer impedance match the measured transfer impedance as good as possible: $m = 300$ nH/m, $l = 7$ μH/m and $c = 600$ pF/m.

4.4 Discussion

This section discusses the transfer impedance measurement results. The first part of this section discusses subjects applicable to both coils. After that, subjects specific for each coil are discussed separately.

4.4.1 Both coils

The sensitivity criterium is 1 V/A. For the major part of the frequency range (above 2 – 3 MHz), the measured transfer impedances are above this value.

Both coils have one or more resonances that can not be explained by the equivalent circuit. Other measurements (not presented in this report), with the same coils on the same test set-up, showed resonances at a different frequencies. The exact position of the coil in the test set-up, varies between different measurements. Also the cable connecting the network analyser are not in the exact same position every measurement. This is an indication that these resonances are caused by the environment (the test set-up and connecting cables). The (varying) capacitance between the coil and the enclosing brass screen, in combination with an inductance (e.g. the self inductance), may cause resonances. Also, the cables connecting the test set-up to the network analyser may cause resonances. During the measurements standing waves can occur between the screen of a cable and earth. These standing waves can cause dips and peaks.

4.4.2 Rogowski coil 1

In the theory in chapter 2, two equivalent circuits were proposed for a Rogowski coil without earth screen. One with (section 2.3.2) and one without (section 2.3.1) inter-turn capacitance. Depending on the value of this inter-turn capacitance, it can or can not be neglected for the frequency range of interest.

It seems that for the frequency range of interest the inter-turn capacitance can be neglected. A capacitance in parallel with the self inductance leads to a wide dip in the transfer impedance at $\omega = 1/\sqrt{LC}$. But the measurements do not show a wide dip. Furthermore, for frequencies above the resonance frequency, a transfer impedance with inter-turn capacitance should approach $Z_t = j\omega M$, while the measured transfer impedance is flat.

The measured mutual inductance is the same as calculated. The self inductance is about a factor three larger than calculated. For a low number of turns, a lot of flux is present around the wire, contributing to the self inductance. Also the wire itself has a self inductance. When the actual measured values are used to calculate the transfer impedance, the measured transfer impedance is virtually the same as calculated, except for a few resonances.

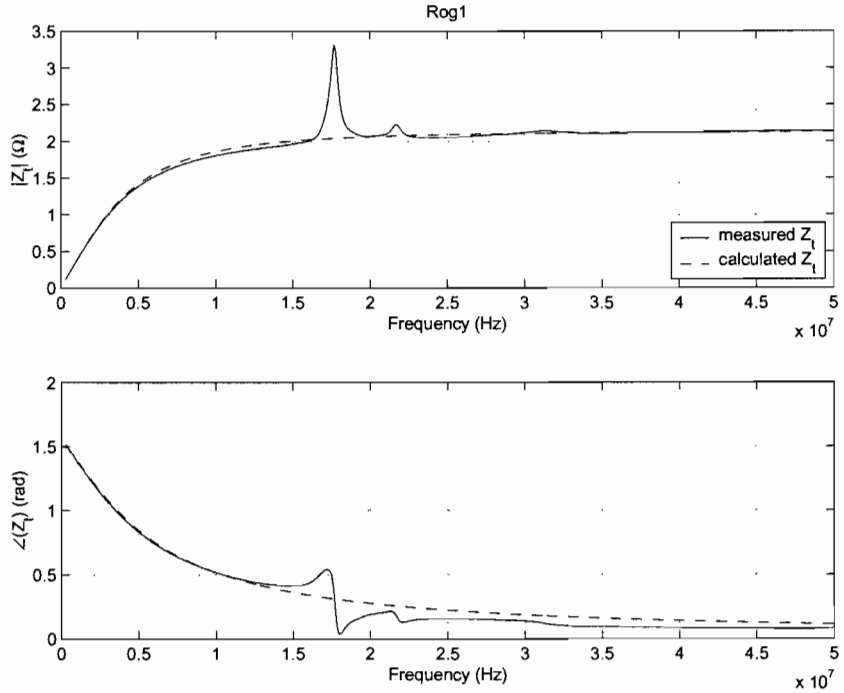

Figure 4.2: Measured and calculated transfer impedance Rog1

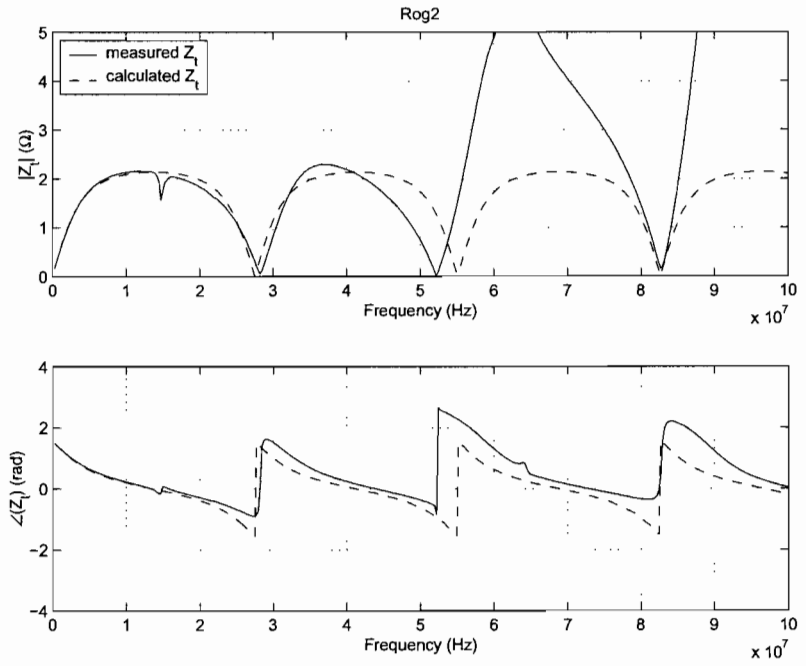

Figure 4.3: Measured and calculated transfer impedance Rog2

For frequencies below the lowest resonance frequency ($\approx$ 18 MHz) both the calculated and the measured curve match very well. The lowest resonance frequency of all measurements is 13 MHz. As states above a slightly different environment changes these resonances. For frequencies below approximately 10 MHz the influence of the environment seems to be negligible.

4.4.3 Rogowski coil 2

The measurements on Rog2 show that the expected repeating pattern of discrete notch frequencies occurs. There is a dip in the transfer impedance approximately every 30 MHz. The lowest notch frequency is lower than expected, because the self inductance is larger than calculated.

The mutual inductance is given by $M = m \cdot G$. The measured mutual inductance is: $M =$ 78 nH. This is larger than calculated, because the winding cross section is larger, since the turns are slightly round.

The measurements show a small dip at 15 MHz. Other measurements (not plotted in this report) show the dip at other frequencies or a small peak, instead of a dip. It seems that this dip is caused by the coil in interaction with the environment, as explained above. Above 10 MHz, the environment and the rest of the measurement system have an unknown influence on the transfer impedance. Because in a practical situation, the transfer impedance is unknown above 10 MHz, it can not be used to accurately measure higher frequencies.

Comparing the amplitude of the dip for both coils, it appears that the dip is much smaller for the screened Rogowski coil. Although this small dip is limiting the use of this coil, the screening seems to quite effective in reducing the resonance. The resonances are an interaction between coil and environment. The screening reduces the effect of the environment and thus reduces the resonances.

Chapter 5

Electrical shielding

The Rogowski coils will be used in an RMU. An RMU is an environment with numerous disturbing electrical and magnetic fields. The coil is clamped around a conductor to measure the current through the conductor. For correct measurement the signal should only couple in inductively. The signals may not couple in capacitively directly from the conductor to the coil or from a nearby conductor to the coil. Also radio broadcast stations can disturb the measurement. To suppress all these disturbances, the Rogowski coil has to be shielded.

5.1 Measuring electrical shielding effectiveness

The Rogowski coils must be shielded against external electric fields. To test the effectiveness of the different shields a shielding test is required. The question that needs to be answered is: given an external electric field, how much signal can be seen at the output terminals of the coil? This question must be answered for both coils in such a way that the results are reproducible and comparable.

5.1.1 Electrical shielding aspects

There are two aspects that contribute to the shield effectiveness:

1. How much current couples in given an external electric field? This can be expressed in the ratio: I_{inj}/E_{ext} where I_{inj} is the injected current and E_{ext} the externally applied electric field. The impedance between the coil and an external electrode is $Z_{ec} = V_{ext}/I_{inj}$, where V_{ext} is the voltage between coil and electrode. When the electrode is kept at the same distance the voltage E_{ext} is proportional to V_{ext}. Thus the impedance between electrode and coil (mainly a capacitance) is a measure for this aspect.

2. How much signal can be seen at the output terminal of the coil given an injected current: $Z_{secinj} = V_{sec}/I_{inj}$? This aspect depends on where the current is injected in the coil. E.g. when the current is injected close to the earth winding most current will flow to earth without causing a voltage at the output. But when the current is injected at the other side of the coil, most current will flow through the conductor (of the coaxial connector) and causes a signal at the output.

5.1.2 Test set-up

In an RMU most disturbing signals couple in from the enclosed conductor, because this is the closest conductor. Therefore a test set-up that simulates this situation is developed. An electrode is placed vertically on a wooden board. The electrode is a hollow brass pipe with an inner diameter of 50 mm, an outer diameter of 52 mm, and a length of 100 mm. Next to the electrode a BNC connector is placed on the board. The conductor of the connector is connected with the electrode by a copper wire below the board. The Rogowski coil that needs to be tested is placed around the electrode. See figure 5.1 for a drawing of the test set-up.

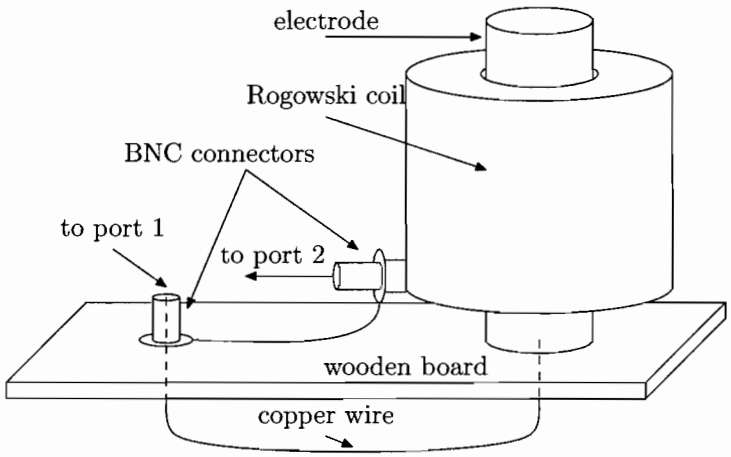

Figure 5.1: Electrical shielding test board

5.1.3 Measuring with the test set-up

With the test board, both electrical shielding aspects can be measured. The coil is placed around the electrode. By means of insulating support the coil is vertically aligned in the middle of the coil. The test board connector is connected to port 1 of a network analyser and the Rogowski coil is connected to port 2 of the network analyser. A wire is connected between the screens of the test board connector and the coil connector. This situation is drawn in figure 5.2. In this figure an inductance L_{loop} is drawn to represent the inductance of the loop (test board connector – electrode – coil – test board connector). The parasitic parallel capacitance C_{par} is in parallel with the electrode and coil. C_{ec} is the capacitance between electrode and coil. This capacitance is a measure for aspect 1.

With the network analyser, the S-parameters S_{11} and S_{21} are measured. S-parameters are the reflection and transmission coefficients between incident and reflection waves for a network with 1 or more ports. S_{11} is the ratio of the reflected wave to the incident wave on port 1. S_{21} is the ratio of the output of port 2 to the incident wave on port 1. These S-parameters can be converted into the input impedance $Z_i = V_1/I_1$ and the transfer impedance $Z_t = V_2/I_1$. Because of the presence of L_{loop} and C_{par} the measured Z_i does not directly correspond with Z_{ec} (C_{ec} in series with coil impedance). Likewise, Z_t does not correspond with Z_{secinj}. Section 5.1.5 describes how

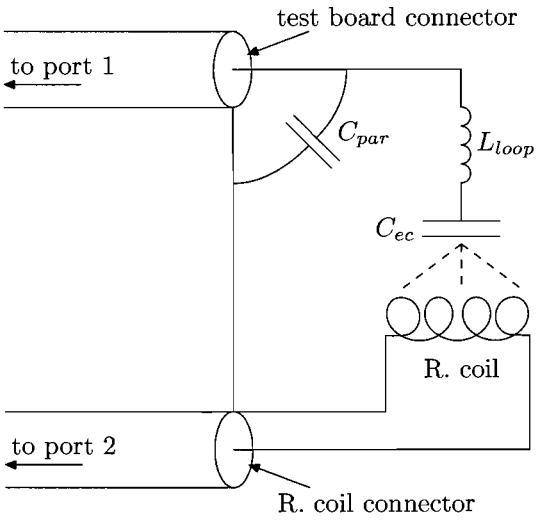

Figure 5.2: Circuit for the testing of both aspects

these quantities can be derived from the measured impedances. First the values for L_{loop} and C_{par} need to be measured with a calibration measurement (see section 5.1.4).

5.1.4 Calibrating the test set-up

The test set-up itself also has an influence on the measurements. It has a parasitic parallel capacitance C_{par} and the loop of the set-up has an inductance L_{loop}. The main reason to fix the electrode and connector on the board, is to make sure that this capacitance and inductance are constant. When they are constant they can be measured before the actual measurements. Afterwards they can be used to compensate the parasitic effects in the actual measurements.

The calibration measurement is as follows. The coil is removed from the test board. A copper wire is connected from the electrode to the screen of the connector. This wire must be placed such that the loop is about the same as with the measurements described earlier in section 5.1.3. The impedance of the test set-up now consists of two parallel elements: C_{par} and L_{loop}. The input impedance of this test set-up is measured.

For low frequencies the impedance of the inductance is much smaller than the impedance of the capacitance. The value of L_{loop} can be determined with the lower frequency range. At higher frequencies C_{par} is significant. At the resonance frequency ($\omega = 1/\sqrt{L_{loop}C_{par}}$) the impedance is infinite. With L_{loop} and the resonance frequency already known, the value for C_{par} can be calculated. When the resonance frequency is outside the measured range C_{par} can be determined with a curve fit in the higher frequency range. In figure 5.3 the measured impedance and the impedance of an ideal parallel LC are plotted. The values for the test board are: $C_{par} = 7$ pF and $L_{loop} = 0.38$ μH. Note that the capacitance is extremely small, making it difficult to determine it accurately. Consequently its influence on the results is negligible compared to the influence of L_{loop}.

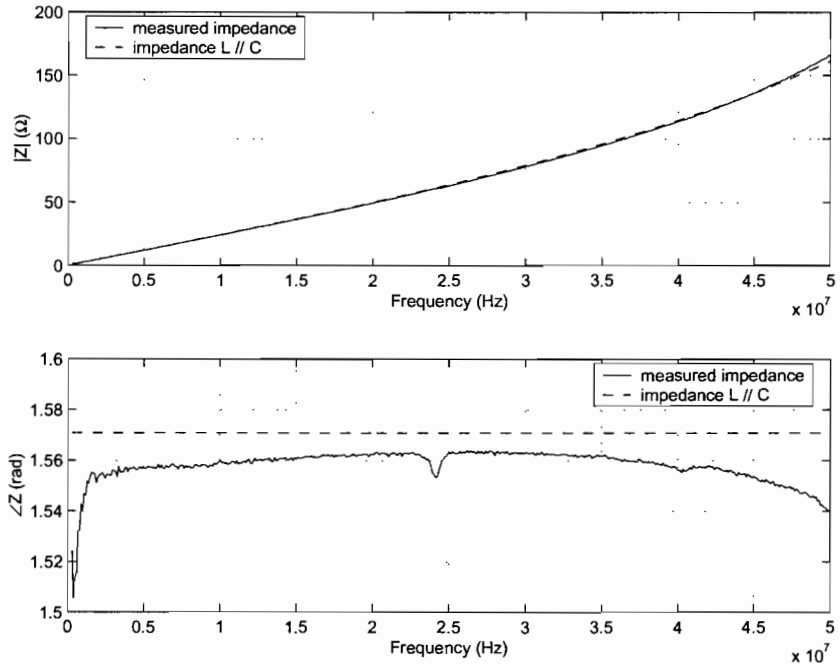

Figure 5.3: Calibration measurement, measured impedance and calculated parallel LC impedance

5.1.5 Interpreting experimental measurement results

The measured input impedance Z_i and transfer impedance Z_t are not directly the required impedances. They need to be corrected for the impedances of the test set-up.

Aspect 1

The first aspect can be measured by measuring the input impedance of port 1 with the set-up as described in section 5.1.3. The coil is connected with a 50Ω coaxial cable with the network analyser. That means that the coil is loaded with 50Ω like in a normal situation. The impedance as seen from port 1 consists of C_{par} in parallel with L_{loop} and C_{ec} in series. See figure 5.4.

The measured input impedance Z_i can be converted into the required impedance Z_{ec} after correction for L_{loop} and C_{par}. Z_{ec} is calculated from Z_i as follows:

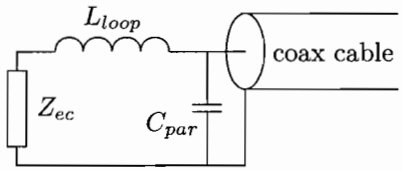

Figure 5.4: Equivalent circuit for aspect 1

$$\frac{1}{Z_i} = \frac{1}{Z_{Cpar}} + \frac{1}{Z_{Lloop} + Z_{ec}} \quad \Rightarrow \quad Z_{ec} = \frac{1}{\frac{1}{Z_i} - \frac{1}{Z_{Cpar}}} - Z_{Lloop} \tag{5.1}$$

Where Z_{Lloop} is the impedance of L_{loop} and Z_{Cpar} the impedance of C_{par}.

Aspect 2

The second aspect is $Z_{secinj} = V_{sec}/I_{inj}$. It tells how much signal can be seen on the output terminals of the Rogowski coil given an injected current. The measured transfer impedance $Z_t = V_2/I_1 = V_{sec}/I_1$ is not the same as Z_{secinj} since C_{par} is present in parallel with the coil. That means that the current I_1 is not the same as I_{inj}.

$$I_{inj} = I_1 \frac{Z_{Cpar}}{Z_{Cpar} + Z_{ecloop}} \quad \Rightarrow \quad I_1 = I_{inj} \frac{Z_{Cpar} + Z_{ecloop}}{Z_{Cpar}} \tag{5.2}$$

Where Z_{ecloop} is the sum $Z_{ec} + Z_{Lloop}$.

The measured transfer impedance can be converted into the required transfer impedance using equation 5.2.

$$Z_t = \frac{V_2}{I_1} = \frac{V_{sec}}{I_{inj}} \cdot \frac{Z_{Cpar}}{Z_{Cpar} + Z_{ecloop}} \quad \Rightarrow$$

$$Z_{secinj} = \frac{V_{sec}}{I_{inj}} = Z_t \cdot \frac{Z_{Cpar} + Z_{ecloop}}{Z_{Cpar}} = Z_t \cdot \left(1 + \frac{Z_{ecloop}}{Z_{Cpar}}\right) \tag{5.3}$$

Total transfer function

Both aspects can be combined into one transfer function. This transfer function tells how sensitive a coil is to a disturbing signal.

$$H = \frac{V_{sec}}{V_{pr}} = \frac{V_{sec}}{I_{inj}} \cdot \frac{I_{inj}}{V_{pr}} = Z_{secinj} \cdot \frac{1}{Z_{ec}} \tag{5.4}$$

5.2 Measurement results

The measurements are conducted on the two Rogowski coils (section 3.6). The unscreened coil with copper wire turns is called Rog1 and the coil with coaxial cable with interruptions in the earth screen is called Rog2. First the test set-up is calibrated as described in section 5.1.4, then the measurements are performed as described in section 5.1.3. Finally the results are processed as described in section 5.1.5 (using the calibration of section 5.1.4). The final results are presented and discussed in this section.

5.2.1 Preliminary measurements

As stated earlier, the location of the torus of the coil where the current is injected is important. Because the diameter of the electrode is quite large, current will be injected all along the coil. But there may still be differences if the electrode moves slightly. To test whether this is the case the electrode is moved inside the coil. The S_{21} parameter is viewed real-time on the screen of the network analyser. If this parameter changes with the position of the electrode, the measurement will not be easily reproducible. The measurements showed for both tested coils that the S_{21} parameter did not change visibly.

5.2.2 Aspect 1

In figure 5.5 the impedance Z_{ec} is plotted for both coils. The measured impedance is as expected mainly capacitive ($Z_{ec} \approx \frac{1}{j\omega C}$). Here, the capacitance C is the capacitance C_{ec} between electrode and coil. The capacitances for Rog1 and Rog2 are $C_{ec1} = 19$ pF and $C_{ec2} = 46$ pF.

The capacitance for Rog2 is higher because the turns are closer to the electrode than the turns of Rog1. The coaxial cable is not as flexible as the copper wire. Therefore the turns are somewhat round and in the middle they (almost) touch the electrode. A second reason for the higher capacitance is that the coaxial cable is thicker than the copper wire. Therefore the surface is larger and thus the capacitance is larger.

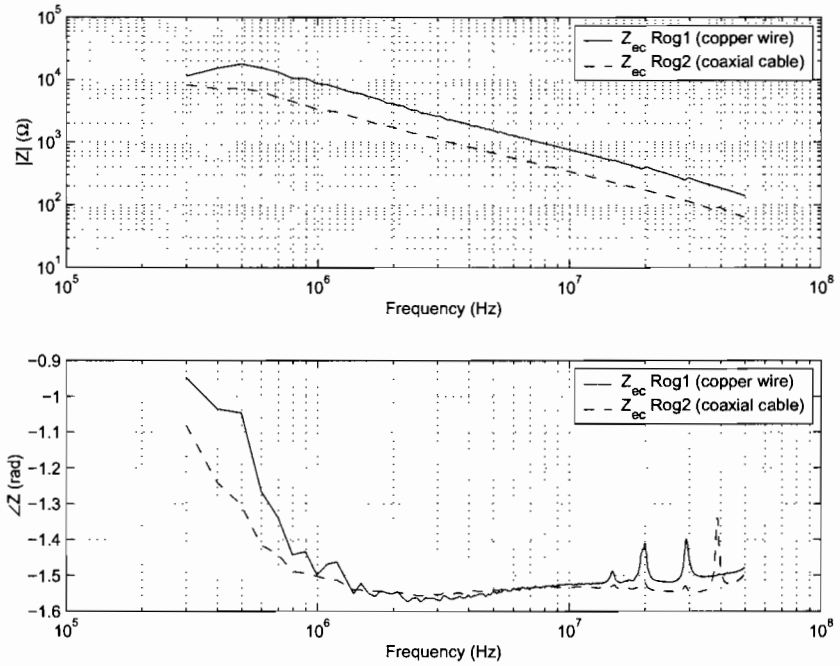

Figure 5.5: Measured impedance $Z_{ec} = \frac{V_{pr}}{I_{inj}}$

5.2.3 Aspect 2

In figure 5.6 the second aspect (Z_{secinj}) is plotted for both coils. The impedance of Rog2 is almost five times smaller than Rog1. That means that the same injected current causes a much smaller voltage at the output. This is as expected since the coaxial cable has an earth screen.

The current that couples capacitively to the coil flows through the electrode. Because the coil encloses the electrode, the coil also encloses this current. Thus, the current also couples inductively to the coil, causing a signal at the output. Z_{secinj} can be split:

$$Z_{secinj} = \frac{V_{sec}}{I_{inj}} = \frac{V_{cap}}{I_{inj}} + \frac{V_{ind}}{I_{inj}} \tag{5.5}$$

Where V_{cap} is the voltage at the output terminals, caused by the capacitively coupled current. And V_{ind} the voltage at the output terminals, caused by the inductive coupling.

Assuming that the current coupling to the coil is distributed homogeneously along the electrode, the current that couples inductively to the coil is $0.5I_{inj}$. To correct Z_{secinj} for this inductive coupling, $0.5Z_t$ has to be subtracted from Z_{secinj}. For Rog1 $0.5Z_t \approx 1/20 \cdot Z_{secinj}$ and for Rog2 $0.5Z_t \approx 1/4 \cdot Z_{secinj}$.

Another thing worth highlighting is the dip at 30 MHz for Rog2. This dip is probably caused by a standing wave in the coil, comparable with the dips in the transfer impedance (see section 2.3.3 and section 4.3).

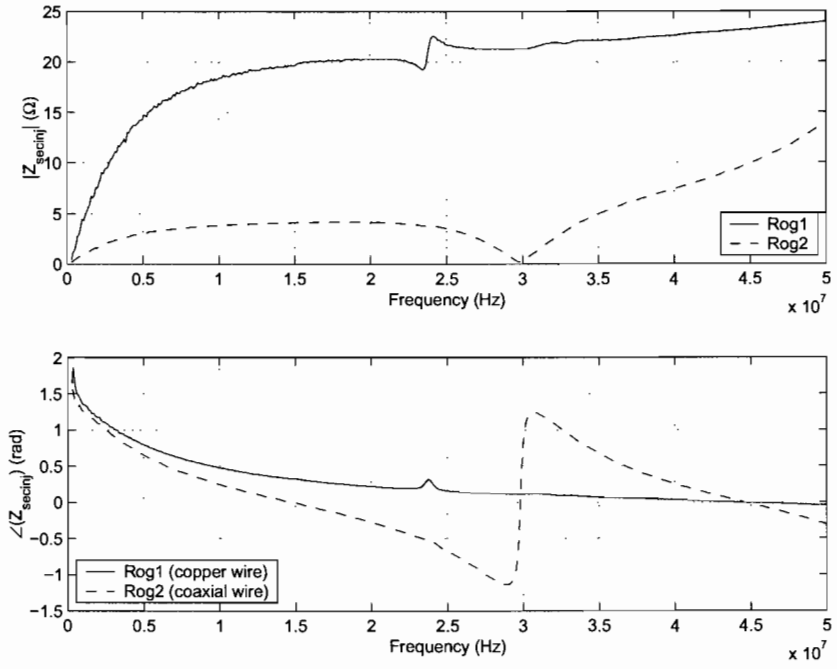

Figure 5.6: Measured impedance $Z_{secinj} = \frac{V_{sec}}{I_{inj}}$

5.2.4 Total transfer function

Aspect 1 and aspect 2 can be combined into one transfer function $H = V_{pr}/V_{sec}$. The results are presented in figure 5.7. The transfer function for Rog1 is about twice as high as Rog2 for frequencies below 30 MHz. At 45 MHz both transfer function are equal and above that the transfer function of Rog2 is higher. Apparently the shielding is less effective above approximately 35 MHz. For high frequencies, aspect 1 is dominant for the shielding effectiveness. However, the coil will not be used above 30 MHz.

The measurements show that Rog2 with the coaxial cable indeed has a better shielding that Rog1 without earth screen. The shielding will be further improved when turns are straight and do not touch the conductor. When the inner diameter of the Rogowski coil is increased the

turn cross section decreases and thus the sensitivity (V_{sec}/I_{pr}) decreases. The best diameter is a trade-off between these two.

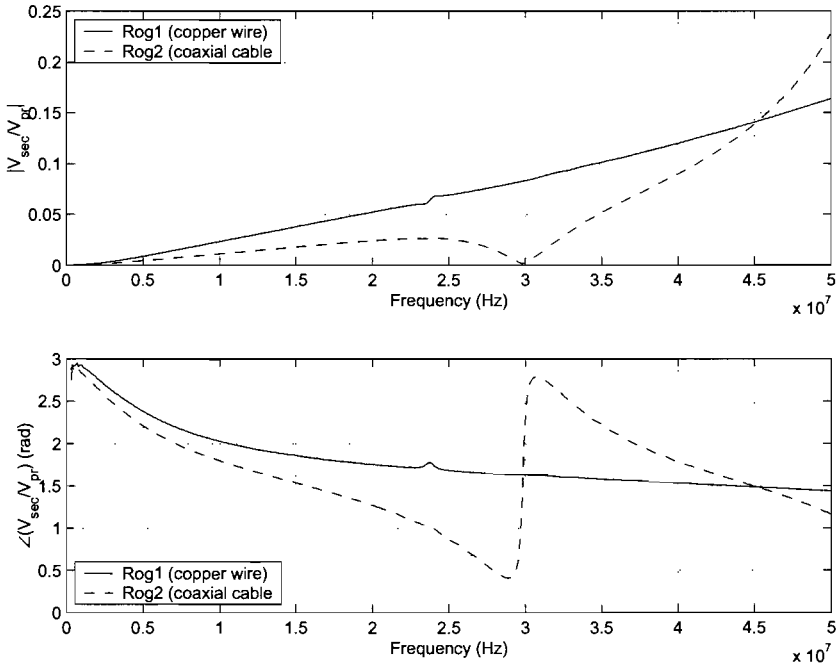

Figure 5.7: Transfer function $H = \frac{V_{sec}}{V_{pr}}$

Chapter 6

Directional sensing

Partial discharges not coming from the cable under test must be discarded. If the direction of the travelling pulse is known, it is known whether the pulse comes from the cable under test or from another source. If only the current and not the voltage of a pulse is measured it is not possible to determine in which direction the pulse is travelling. A positive pulse travelling in one direction and a negative pulse travelling in the opposite direction result in the same current polarity. Therefore additional measurements are required to determine the pulse direction.

In the past, several methods were described to detect the direction of a travelling wave. For example the directional coupling sensor described in [Oli54]. In [Pom99] several methods applied in cable accessories are summarised. Unfortunately, none of these sensing methods can be applied because they require an alteration of the circuit, which is impossible without taking the cable off-line. One interesting method is described in [Wen95], an inductive and capacitive sensor are combined to produce a directional sensor. Because a capacitive divider is used, this technique can not be applied without taking the cable system off-line either.

This chapter discusses two methods that can detect the direction of the pulses: Polarity-of-First-Peak sensing (PFP) and directional and differential sensing (DirecDiff).

6.1 KEMA test set-up

At the KEMA premises in Arnhem (the Netherlands) a test set-up is build for the PD online project. The test set-up consists of two real RMUs with transformers and 300m 10kV PILC cable in between. There is a joint half way this 10kV cable. Recently a second 10kV cable was added to the test set-up. This XLPE cable starts at RMU 2 and loops back to another Magnefix (switchgear) in the same RMU. This cable also has a joint in the middle. The transformer in RMU 2 is connected to Magnefix 1. A schematic drawing of the test set-up can be found in figure 6.1.

In this chapter abbreviations and symbols are used for different parts and locations in an RMU. Their meaning can be found in appendix A.

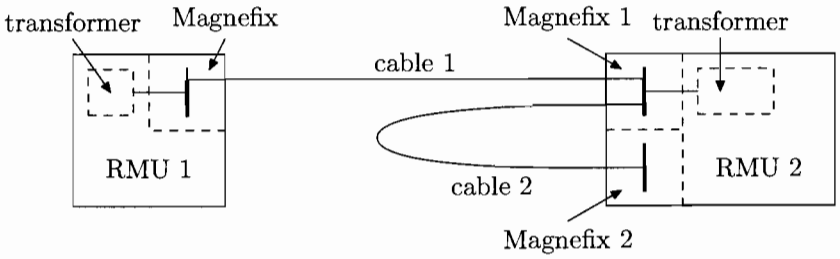

Figure 6.1: KEMA test set-up

6.2 Polarity-of-First-Peak sensing

6.2.1 Theory

The magnetic field H around a conductor is proportional to the current through the conductor. Together with the electric field E the magnetic field gives the Poynting vector according to:

$$\vec{S} = \vec{E} \times \vec{H}$$

The direction of the Poynting vector is the direction of the energy flow and thus the direction of the pulse. As pointed out above, the direction of the magnetic field H is directly related to the direction of the current. Likewise, the direction of the electric field E is directly related to the polarity of the voltage. When the voltage and current of the pulse are known, the direction of E and H are known and the direction of the pulse can be derived.

Unfortunately, it is not possible to measure the voltage directly because the power delivery would have to be interrupted in order to install a voltage sensor. Instead, the voltage can be reconstructed by measuring the current through another impedance in the RMU. The measured current multiplied by the impedance gives the voltage across the impedance. If this impedance is in parallel with the incoming cable under test, this is also the voltage across the cable. The voltage over and the current through the cable are multiplied to get the power of the pulses in the cable. This way the direction of the pulses can be determined.

In an RMU the impedances can be modelled as a combination of resistors, inductances and capacitances. Consider a current pulse that starts with a half cycle of a sine wave (see figure 6.2). The current before $t = 0$ is zero and after $t = 0$ the current increases to a maximum and decreases again. Because before $t = 0$ the current is equal to zero (in an ideal situation), it is possible to determine whether the voltage across an impedance is positive or negative directly after $t = 0$, without knowing the exact impedance (assuming the impedance is positive). The voltage across a resistor, a capacitance and an inductance are given by: $v_R = Ri_R$, $v_C = \frac{1}{C}\int i_C\,dt$ and $v_L = L\frac{di_L}{dt}$. All three voltages have the same sign as the current directly after $t = 0$ for the current as in figure 6.2 (assuming $v_C = 0$ at $t = 0$). This means that the sign of the voltage across an impedance directly after the beginning of the pulse is the same as the sign of

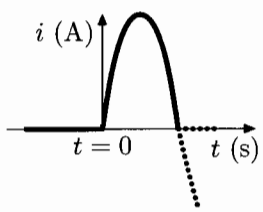

Figure 6.2: Example pulse

the current through the impedance. This also means that the polarity of the first current peak is the same as the polarity of the first voltage peak.

If the polarity of the first peak of both the current and the voltage are known, the polarity of the first peak of the power is known as well and thereby the direction of the pulse. When the polarity is the same (either both positive or both negative) the pulse travels in one direction and when the polarity is different the pulse travels in the other direction. This way the polarity of the first peak of both measured currents defines the pulse direction. The difference in polarity is also explained in a different way in section 6.3. See also figure 6.6.

In the theory above an important assumption is made: the second impedance through which the current is measured is positive. But when a PD comes from this impedance it can no longer be seen as an impedance. It is a current source producing the pulse. Therefore only impedances that do not produce PDs themselves can be used as a second sensor location for directional sensing. In an RMU, the only component that does not produce PDs is the short XLPE cable, being the impedance between the conductor of the cables to the transformer and earth (Z_{tcce}). Other 10kV cables and the transformer are possible PD sources.

6.2.2 Measurements

In order to verify the theory from section 6.2.1, measurements were done at the KEMA test set-up (see figure 6.1). In RMU 2 there are two incoming 10kV cables. In RMU 2 a current probe is attached PLEC 10kV cable 1 and another around earth TCC (see appendix A for an explanation of these locations in an RMU). The direction of both probes is the same. Cable 1 is the cable under test. Two pulses are injected at the far side of the cable under test and two pulses are injected at the far side of other cable (cable 2) and another around 3 TCC. Injecting around 3 TCC represents a pulse coming from the transformer. If the theory above is correct, the polarity of the first peak of both currents is different for the pulses from cable 1 and the same for the pulses from cable 2 and the transformer.

Three different situations were investigated. For all measurements the currents i_1 and i_{tcce} were recorded.

Figure 6.3 A positive and negative incoming pulse from the cable under test. The polarity of the first peak of both currents is opposite for both the positive and the negative pulse. This is as expected for an incoming pulse.

Figure 6.4 Positive and negative pulse from the cable *not* under test. This is an outgoing pulse. The polarity of the first peak of both currents is the same for both the positive and the negative pulse. This is as expected for an outgoing pulse.

Figure 6.5 A pulse from the direction of the transformer. This is an outgoing pulse. The polarity of the first peak of both current is the same. This is as expected for an outgoing pulse.

Figure 6.3 shows the measured currents for incoming pulses. The pulse arriving from the cable is the large peak just after $t = 11$ μs. Prior to this pulse there are some small oscillations. These signals can not be the pulse arriving from the cable since they arrive too fast after the injection pulse (the injection pulse is not drawn in the figure). The two measured currents were recorded with one digitiser. The signals of the injected current and the primary current were not connected

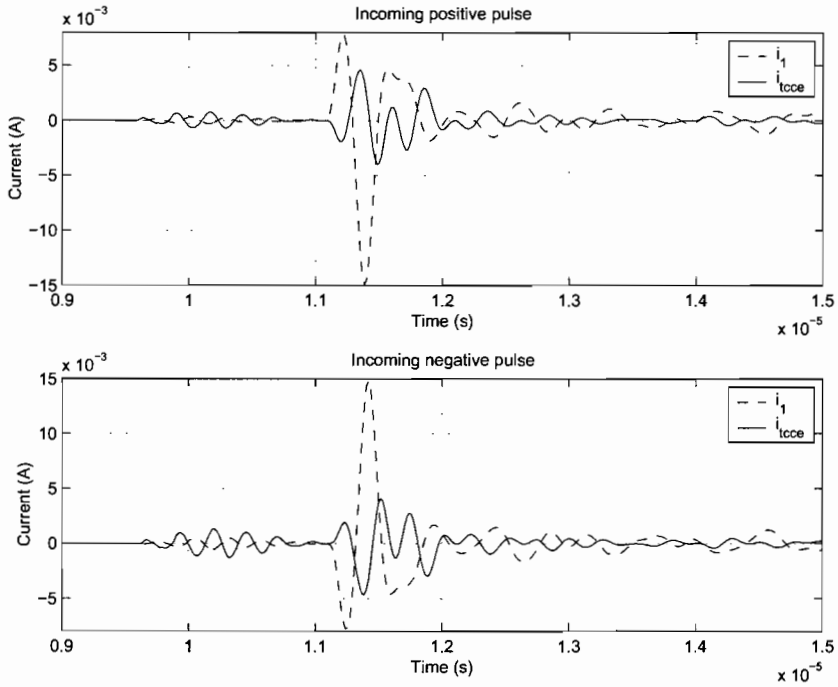

Figure 6.3: A positive and negative pulse from the cable under test (cable 1)

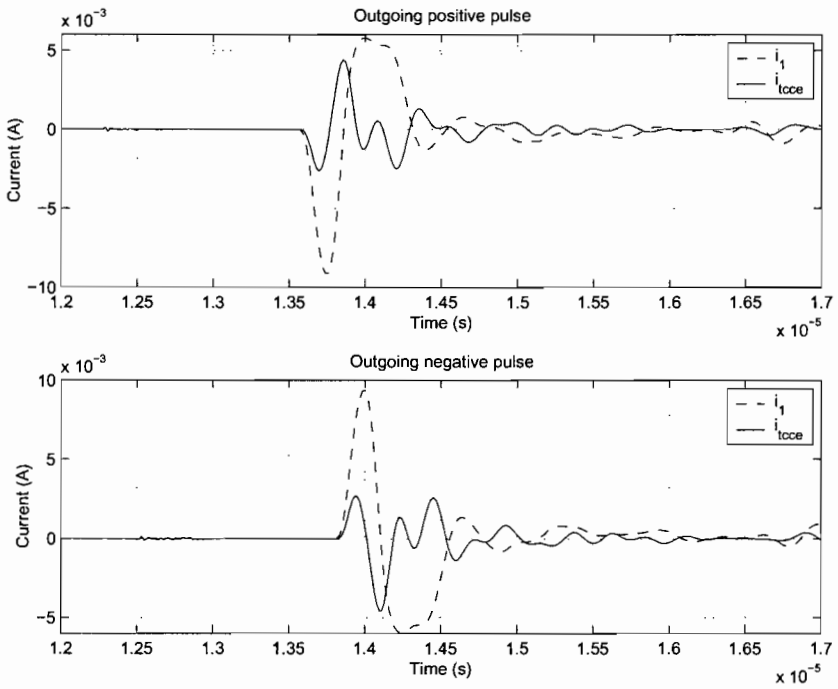

Figure 6.4: A positive and negative pulse from the cable *not* under test (cable 2)

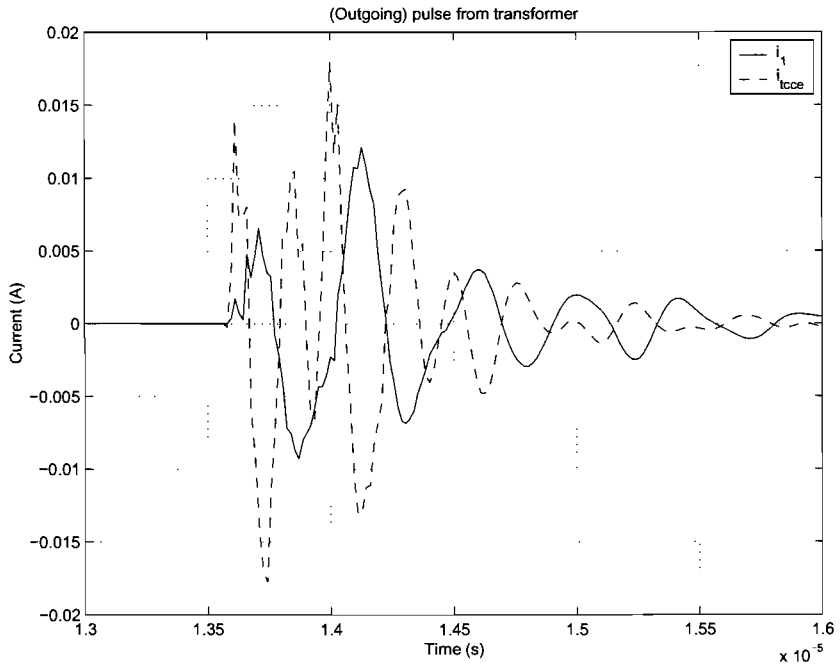

Figure 6.5: A pulse from the direction of the transformer

to the digitiser at the time of the measurement. That means that cross-talk between channels can not be the cause of the oscillations.

Because the speed of a pulse through a cable is approximately $2 \cdot 10^8$ m/s and the cable length is 300 m, the pulse arrives 1.5 μs after the injection pulse. But the first oscillations are sooner. The injection coil also acts as an antenna. The EM waves through the air travel with $3 \cdot 10^8$ m/s and the two RMUs are only 20 m apart (the cable is on a reel). The circuit picks up these EM waves in the air, causing a small signal. Another possibility is that the signal is picked up by the CM circuit of the measuring system.

6.2.3 Discussion

The Polarity-of-First-Peak (PFP) directional sensing method works very satisfactory. Measurements showed that on the KEMA test set-up with two real RMUs the method can accurately determine the direction of the injected pulses.

It is obvious that the major advantage of the PFP technique is that the impedance does not need to be known (as long as it does not produces PDs itself). But this technique also implies that only the direction of the pulse is determined. There is no extra information about the power and energy of the pulse. The voltage can be calculated when the impedance is known exactly. It can be multiplied with the current through the cable i_{plec} to get the instantaneous power. This power integrated over time gives the energy. But in case that it is not necessary to have information about pulse power and energy the easy PFP technique is sufficient.

Determining the polarity of the first peak for both current signals separately and determining the pulse direction afterwards has the advantage that a different time shift for both channels is no complication. The signals are only shifted in time, the polarity does not change.

A disadvantage of this PFP method is that in case of two different pulses (from two different sources/defects), the pulses must be clearly separated from each other. If an incoming pulse and an outgoing pulse overlap (partially or completely) the combined signal can mistakenly be interpreted as either an incoming or outgoing pulse. The directional sensing method described in section 6.3 does not have this disadvantage. Also a low signal-to-noise ratio can result in incorrect signal interpretation.

The misinterpretation of the pulse direction is not necessarily a problem for the analysis of the cable state. The chance that an incoming and an outgoing pulse overlap is random. When a pulse is mistakenly interpreted as an outgoing pulse, it will be ignored. That means that an incoming pulse is ignored, while it should not have been ignored. But because the occurrence of double pulses is completely random, this is no problem for the analysis of the state of the cable. When a double pulse is interpreted as an incoming pulse, the pulse is interpreted as an incoming pulse with a different charge than actual incoming pulse. The pulse is measured at both ends of the cable. In such a situation, the ratio of the pulse charge measured at one end, to the pulse charge measured at the other end of the cable, is different than expected and the pulse can be discarded.

6.3 Directional and differential sensing

6.3.1 Theory

When a pulse coming from a 10kV cable enters an RMU, the current distributes over the impedances in the RMU. The direction of the current through each impedance depends on were the pulse enters the RMU. Consider figure 6.6(a). In this figure a pulse enters the RMU through 10kV cable 1. The direction of the current through the other impedances is drawn in the figure. The direction of some currents is different if the pulse comes from 10kV cable 2 (Z_2), see figure 6.6(b). See appendix A for more information on the impedance symbols.

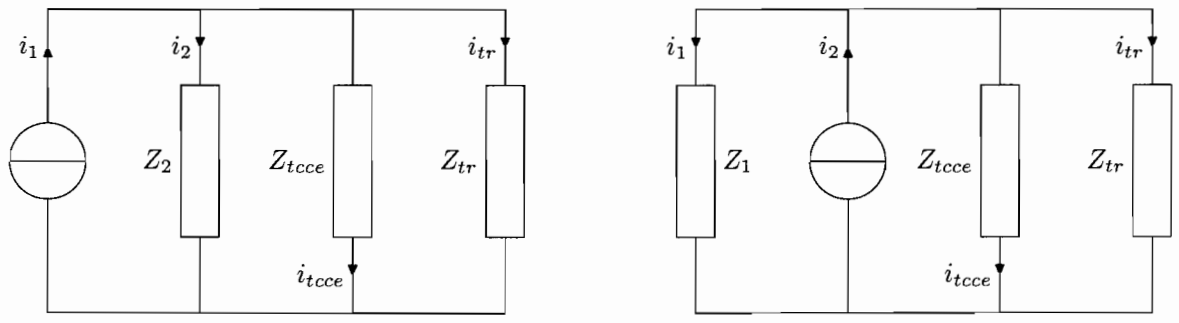

(a) Pulse coming from 10kV cable 1

(b) Pulse coming from 10kV cable 2

Figure 6.6: Current directions when the pulse comes from 10kV cable 1 (left) or 2 (right)

In the first situation (a pulse from 10kV cable 1), the direction of the currents i_1 and i_{tcce} are opposite. In the second situation the direction of these two currents is the same. Consider the situation that cable 1 is under test, then pulses from cable 1 are incoming pulses (as seen from the RMU looking at the cable under test) and pulses from cable 2 and the transformer are outgoing pulses. If the transfer function from i_{tcce} to i_1 is known, a measured i_{tcce} can be converted into i_1. This transformed current and the measured i_1 can be subtracted:

$$I_1 - H_{tcce,1} \cdot I_{tcce} = \begin{cases} I_1 - -I_1 = 2I_1 & \text{if incoming pulse (from cable 1)} \\ I_1 - I_1 = 0 & \text{if outgoing pulse (from cable 2 or transformer)} \end{cases} \tag{6.1}$$

Where $H_{tcce,1}$ is the transfer function from I_{tcce} to I_1.

The resulting signal only contains the pulses incoming from cable 1 and no pulses from other sources. In this way directional sensing is achieved without determining the direction of each pulse separately. But this method has another advantage, it is a differential measuring technique. That means that any disturbance signal that causes a current through both Z_1 and Z_{tcce} in the same direction is automatically removed from the resulting signal because of the subtraction.

Unfortunately there is one complication. The transfer function $H_{tcce,1}$ depends on the direction of the pulse. In other words, the direction of the pulse has to be known before the right transfer function can be used. Using equation 6.1 and figure 6.6 the following can be derived:

$$H_{tcce,1} = \begin{cases} H_{tcce,1,in} = \frac{-I_1}{I_{tcce}} = \frac{Y_{tcce}+Y_2+Y_{tr}}{Y_{tcce}} & \text{for incoming pulses} \\ H_{tcce,1,out} = \frac{I_1}{I_{tcce}} = \frac{Y_1}{Y_{tcce}} & \text{for outgoing pulses} \end{cases} \tag{6.2}$$

Where $Y_{..}$ is the admittance of the circuit component $Z_{..}$. The subscripts $_{in}$ and $_{out}$ give the direction as seen from the RMU looking at the cable under test. Note that if the admittance of both 10kV cables are equal and dominant, both transfer functions are about equal.

If the transfer function for outgoing pulses is used in equation 6.1, the resulting signal is free of disturbing outgoing pulses.

$$I_{filt} = I_1 - H_{tcce,1,out} \cdot I_{tcce} \tag{6.3}$$

Where I_{filt} is the filtered signal.

Incoming pulses that are processed with equation 6.3 will be deformed because the transfer function for outgoing pulses is used. This signal, free of disturbing outgoing pulses, can be used to identify the interesting parts of the signal and then extract these parts from I_1. But if a second transfer function $H_{2,in}$ is used the desired effect can still be reached. Consider equation 6.4, the part between the brackets is the same as in equation 6.3.

$$I_{filt} = H_{2,in}(I_1 - H_{tcce,1,out} \cdot I_{tcce}) \tag{6.4}$$

Where I_{filt} is the resulting filtered signal and $H_{2,in}$ is a transfer function to correct the deformation of incoming pulses.

Multiplying with $H_{2,in}$ has no effect for outgoing pulses because the part between the brackets in equation 6.4 is equal to zero for outgoing pulses. The transfer function $H_{2,in}$ must be chosen such that the deformation of incoming pulses in cancelled. In other words I_{filt} must be equal to

I_1 for incoming pulses. Therefore I_{filt} in equation 6.4 is substituted with $I_{1,in}$. That means that the transfer function must be calculated with a measured incoming pulse. Also I_1 is substituted with $I_{1,in}$ and I_{tcce} with $I_{tcce,in}$ because $H_{2,in}$ is calculated with an incoming pulse. Rewriting the resulting equation results in equation 6.5.

$$H_{2,in} = \frac{I_{1,in}}{I_{1,in} - H_{tcce,1,out} \cdot I_{tcce,in}} = \frac{H_{tcce,1,in}}{H_{tcce,1,in} + H_{tcce,1,out}} \tag{6.5}$$

This function is independent of the current I_1 or I_{tcce} because the transfer functions $H_{tcce,1,..}$ only depend on the impedances (see equation 6.2).

Before the measured signal can be filtered in this way, both transfer functions must be calculated. The transfer function $H_{tcce,1,out}$ must be calculated once for an outgoing pulse and the transfer functions $H_{tcce,1,in}$ and $H_{2,in}$ must be calculated once for an incoming pulse.

6.3.2 Measurements on test board

In order to easily test the directional and differential sensing, a small test board was constructed. The test board is a simple model of a real RMU. The board has four parallel impedances: two 50 Ω coaxial cables (Z_1 and Z_2), resistor simulating the impedance Z_{tcce} and a resistor simulating Z_{tr}. The values of the resistors are chosen such that they have about the same impedance as in a real RMU for frequencies of 1 MHz ($Z_{tr} = 82\ \Omega$ and $Z_{tcce} = 120\ \Omega$). The test board is schematically drawn in figure 6.7.

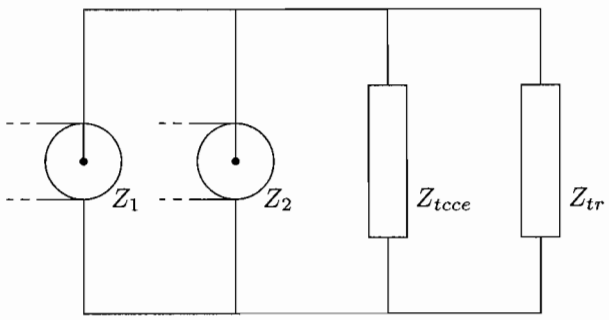

Figure 6.7: Directional and differential sensing test board

Injection at far end

For the first measurements, either single pulses or continuous pulses are injected at the far end of both coaxial cables. A function generator is directly connected to one of the cables. For incoming pulses the function generator is connected at the far end of cable 1. For outgoing pulses the function generator is connected to the far end of cable 2. In both situations the cable where the pulses are not injected is characteristically terminated with 50 Ω. The currents i_1 (cable under test) and i_{tcce} are measured.

The current i_{tcce} is measured with a Tektronix current probe. The current i_1 is measured by directly measuring the voltage over the impedance Z_1. Before the actual measurements a

calibration measurement was conducted. The current i_1 is measured with the current probe and the voltage is measured. The transfer function from the measured voltage to i_1 is calculated. This transfer function is used to convert the measured voltage into i_1 during the actual measurements.

First two calibration pulses (one incoming and one outgoing) are injected to calculate the transfer functions $H_{tcce,1,in}$ and $H_{tcce,1,out}$. These transfer functions are used to calculate $H_{2,in}$. As a calibration pulse a very short pulse (but long enough for the used sample frequency) is used to get a wide frequency spectrum.

These measured transfer functions can be compared with theoretically calculated transfer functions. The impedances of the test board are relatively simple. The resistors and coaxial cable are real impedances. The loops of the wires are modelled as inductions. The inductance of one loop is estimated ($\approx$ 450 nH). This inductance is placed is series with each resistance. For low frequencies (< 17 MHz) the theoretical curve can be matched with the measured curve by adjusting the inductances. But above 17 MHz there are resonances in the measured transfer function that can not be modelled with only a resistor and an inductance. Parasitic capacitances and inductances are responsible for this.

After the calibration pulse, other pulses and signals are injected (both incoming and outgoing). For all these pulses i_{filt} is calculated using equation 6.4. If the theory is correct the outgoing pulses are removed from the clean signal and the incoming pulses are undistorted in the clean signal. In figure 6.8 and 6.9 an incoming and outgoing square pulse are compared. Note that these figures are zoomed in on the interesting part of the signal. The actual sample is much longer to catch the entire signal until all oscillations are damped out. The incoming signal matches very good with i_1 and the outgoing signal is nearly equal to zero.

Injection locally with injection coil

In a practical situation with real RMUs, it takes a lot of effort to inject a pulse at the far end of the cable *not* under test. Someone has to drive to the other RMU and inject a calibration pulse there. This is much easier for the cable under test because an injection coil is installed already at both sides of this cable. This problem can be avoided if a pulse is injected locally with an injection coil around the 10 kV cable PLEC.

The situation with local injection is also tested on the test board. An injection coil is clamped around the conductor above Z_1 for incoming pulses and around Z_2 for outgoing pulses. The currents i_1 and i_{tcce} are measured. These currents are used to calculate the filtered signal i_{filt}. The transfer functions determined with pulses injected at the far end in the last section are used for this calculation. If the theory is correct, i_{filt} is equal to i_1 for (incoming) pulses injected over Z_1 and i_{filt} is equal to zero for (outgoing) pulses injected over Z_2. However, if they do not match, then $H_{tcce,1,in}$ and $H_{tcce,1,out}$ are different for local and far end injection. That means that the injection coil can not be modelled as a simple voltage source and other effects of the coil on the circuit have to be considered.

In figure 6.10 an incoming pulse is filtered and compared with i_1. Both signals match quite well, both the pulse shape and amplitude are similar. But the match is not as good as for pulses injected at the far end, as shown in figure 6.11. (Figure 6.10 and 6.11 are zoomed in on the interesting part of the signal.) Also an outgoing pulse is filtered. The filtered signal should have been equal to zero. Apparently, this is not the case: the amplitude of the filtered is about one

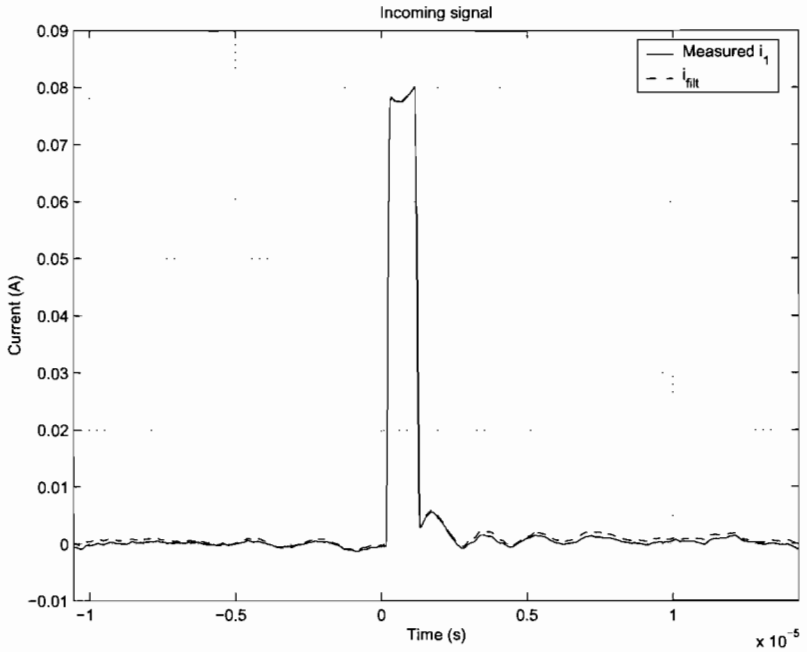

Figure 6.8: Measured i_1 and filtered signal for an incoming pulse injected at the far end (measured on test board)

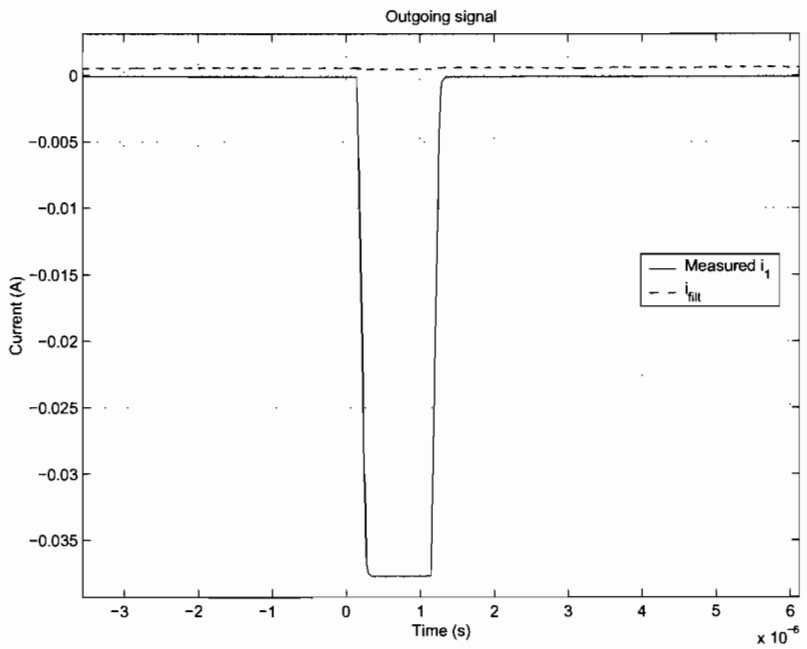

Figure 6.9: Measured i_1 and filtered signal for an outgoing pulse injected at the far end (measured on test board)

third of the i_1. The filtered signal amplitude is reduced but certainly not zero. For a shorter pulse the amplitude appeared to be even higher. For a longer pulse the results match better with the theory.

6.3.3 Measurements on KEMA test set-up

After the measurements on the small test board similar measurements are conducted on the test set-up at KEMA. The cable under test is cable 1. Two current probes are installed in RMU 2 Magnefix 1 around 10kV PLEC 1 and around earth TCC. For all measurements the current probes (Fischer F-70) remain in place while several pulses are injected at various locations in RMU 1 and RMU 2.

Calibration pulses are injected locally at PLEC 10kV cable 1 (in RMU 2, Magnefix 1) and locally at PLEC cable 2 (in RMU 2, Magnefix 1). With the measured i_1 and i_{tcce} the transfer functions are calculated. After that, pulses with various widths are injected locally. With these pulses the calculated transfer functions are tested. For all locally injected PLEC 1 (incoming) pulses, i_{filt} is virtually the same as i_1 (figure 6.12). For all locally injected PLEC 2 (outgoing) pulses, i_{filt} is equal to zero (figure 6.13) . Just as with the measurement on the test board the filtering is very good for locally injected pulses when the sensing method is calibrated with locally injected pulses.

The important question is how well the transfer functions, calculated with local injection, are applicable for pulses injected at the far end. Several pulses with different widths are injected at the far side of both cables. In figure 6.14 i_{filt} and i_1 are plotted for an incoming pulse and in figure 6.15 for an outgoing pulse.

The filtered signal i_{filt} and i_1 match very good for an incoming pulse. In the signal with the outgoing pulse several reflections can be seen. The first pulses travels from RMU 2 to RMU 1 through the cable. It reflects at RMU 1 and travels back to RMU 2. This reflection can be seen as the second larger peak in figure 6.15. This pulse also reflects on RMU 2 going back to RMU 1. This continues until the pulse is damped out completely. The current i_{filt} is almost zero during the first pulses. But during the second pulse (reflection) the filtered signal is almost as large as i_1. Clearly the reflection from RMU 1 is interpreted as a signal coming from the cable under test and will therefore remain as a signal in i_{filt}.

The second 10kV cable (cable 2 on the KEMA test set-up) is not the only source of disturbing PDs. Also the transformer is a possible PD source. Therefore pulses are injected at 3TCC at the KEMA test set-up. Injecting around 3TCC simulates a pulse coming from the transformer. In figure 6.16 i_{filt} and i_1 are plotted. Because a pulse from the transformer is an outgoing pulse i_{filt} should be zero. As can be seen in the figure this is clearly not the case. The amplitude of i_{filt} is larger than the measured i_1.

6.3.4 Discussion

Local and far end injection

The first tests on the test board showed that DirecDiff sensing works very good if calibrated with a short pulse injected at the far end. However, it does not work very well when calibrated by means

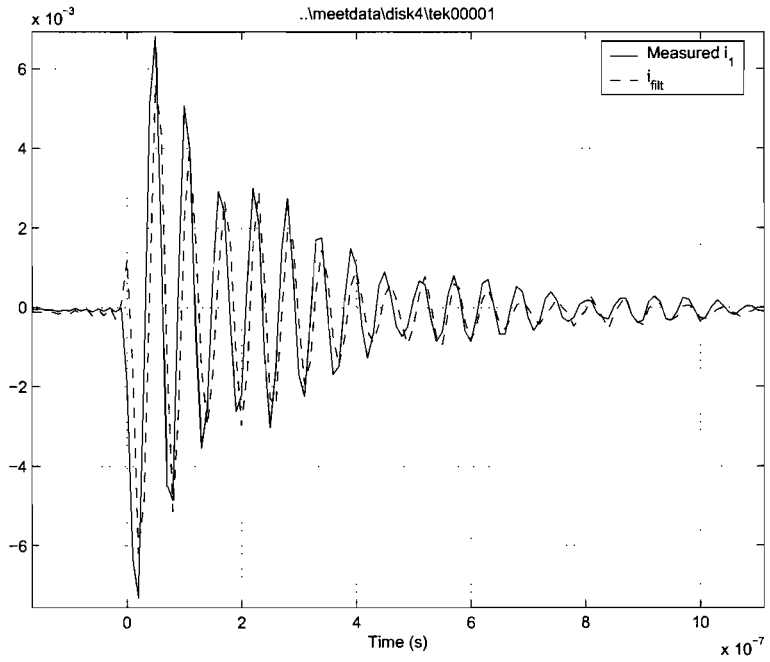

Figure 6.10: Measured i_1 and filtered signal for an incoming locally injected pulse (measured on test board)

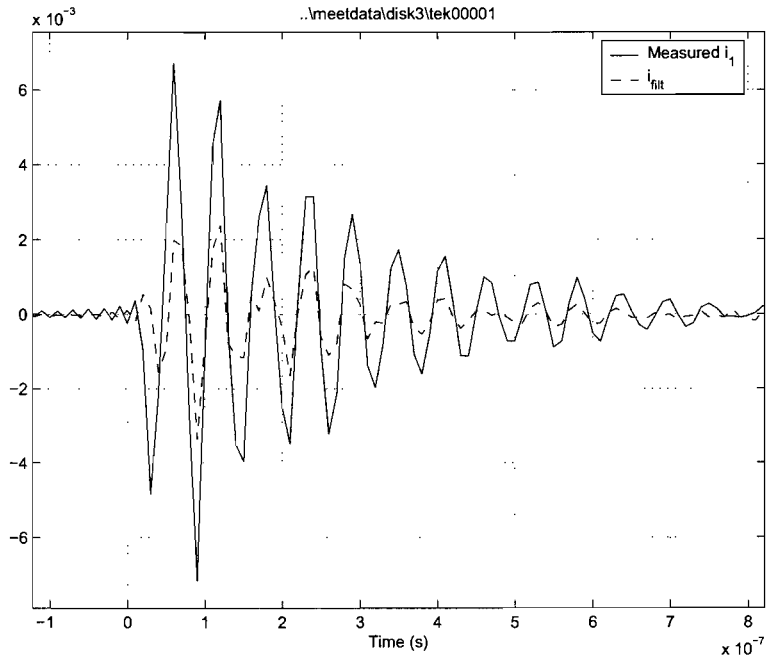

Figure 6.11: Measured i_1 and filtered signal for an outgoing locally injected pulse (measured on test board)

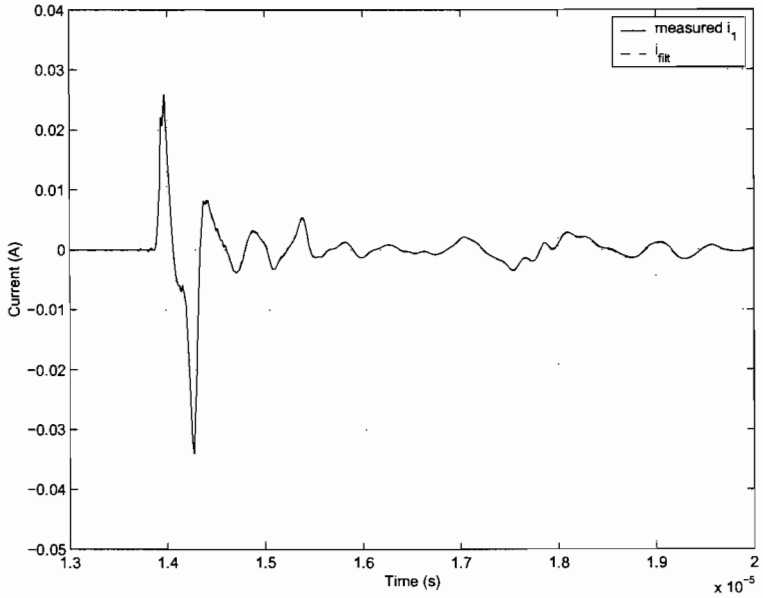

Figure 6.12: i_{filt} and i_1 for an incoming locally injected pulse (measured at the KEMA test set-up)

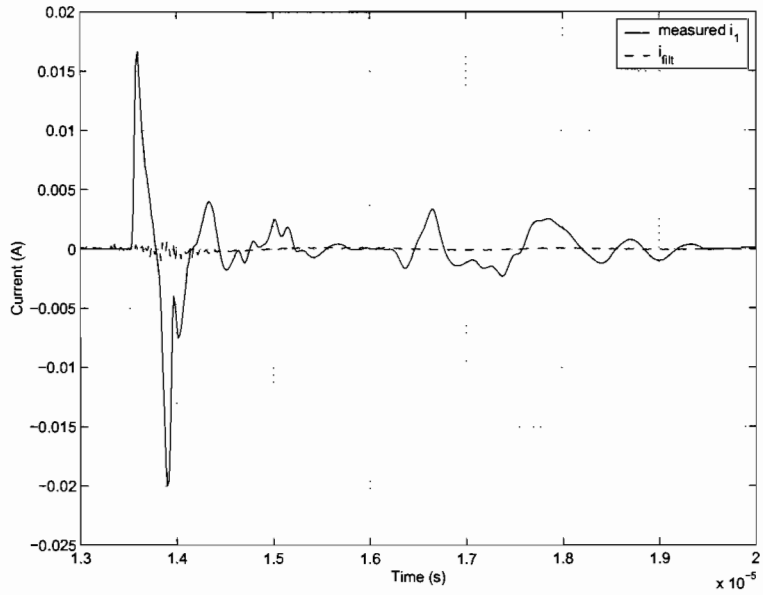

Figure 6.13: i_{filt} and i_1 for an outgoing locally injected pulse injected at the far end (measured at the KEMA test set-up)

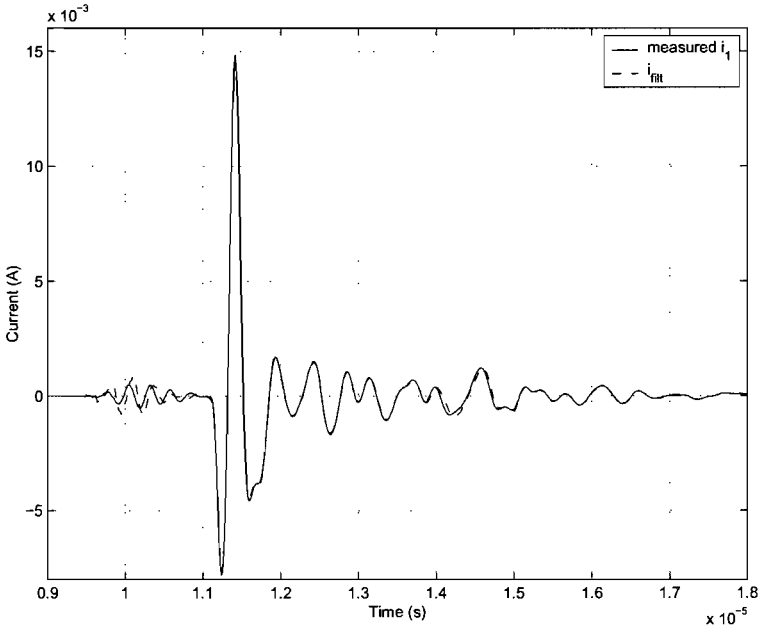

Figure 6.14: i_{filt} and i_1 for an incoming pulse injected at the far end (measured at the KEMA test set-up)

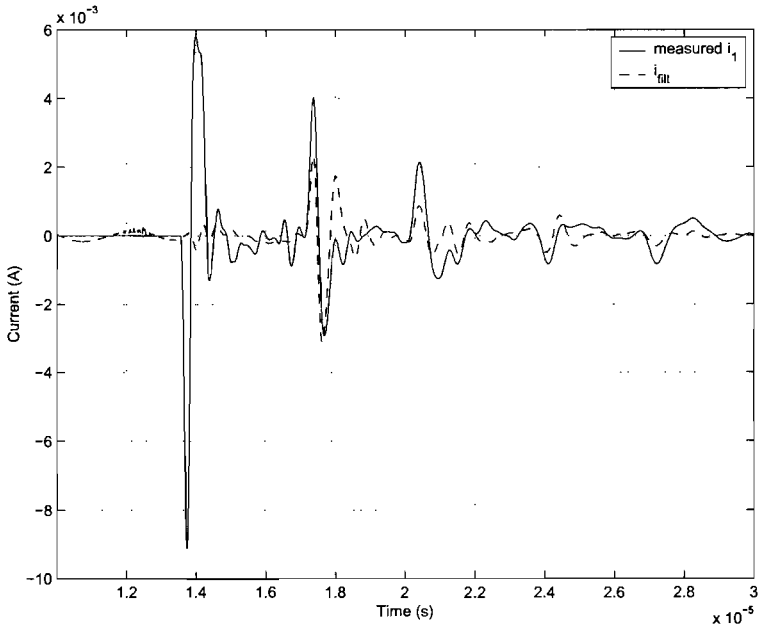

Figure 6.15: i_{filt} and i_1 for an outgoing pulse injected at the far end (measured at the KEMA test set-up)

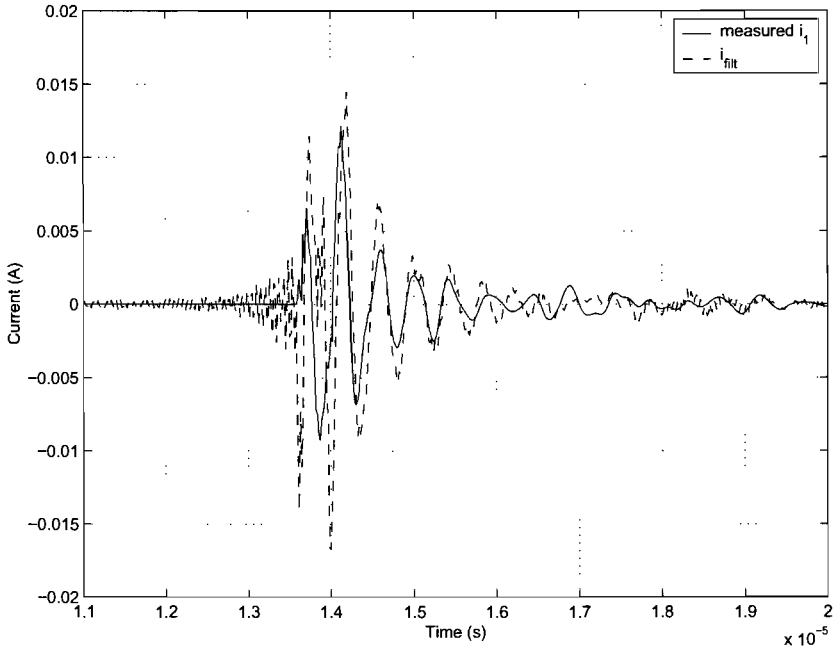

Figure 6.16: i_{filt} and i_1 for an outgoing pulse injected locally around 3TCC (measured at the KEMA test set-up)

of pulses which are injected locally. Apparently the injection coil introduced an extra impedance in the circuit that can not be neglected.

The measurements at the KEMA test set-up showed that DirecDiff sensing works quite well, even when calibrated with locally injected pulses. Apparently the influence of the injection coil on the circuit is much smaller than on the test board. The main difference between the test board and the KEMA test set-up is the size. Also a different injection coil is used. On the test board a current probe with magnetic core is used as injection coil, while at the KEMA test set-up a coil with air core is used. The current probe used for injection on the test board has a transfer impedance of 1–10 Ω (depending on the frequency). The ferromagnetic core of this probe has a $\mu_r \gg 1$. The cross section of the core is approximately 10 cm^2. The cross section of the loops on the test board is about 200 cm^2. That means that the core causes a significant increase in magnetic flux and thus a larger inductance of the loop. Because the inductance is different, the transfer functions $H_{tcce,1,in}$ and $H_{tcce,1,out}$ are changed by installing the coil on the test board.

An alternative calibration method might be to use real PD pulses instead of a pulse injected locally. The PDs need to be clearly separated from each other. Then, the direction of these pulses can be determined with the PFP method and used to calibrate the DirecDiff technique. Because both an incoming and an outgoing pulse are required for the calibration this calibration method can not be used if one of the two 10kV cables does not produce PDs. Further, PDs from inside the RMU may be confusing.

Pulses from the transformer

Pulses injected around 3TCC simulate a pulse coming from the transformer. The filtered signal i_{filt} of these pulses should be equal to zero, but the measurements showed that this is clearly not the case. This can be explained considering a different equivalent circuit (figure 6.17). The original equivalent circuit has four parallel impedances. The transfer function $H_{tcce,1,out}$ is in that case the same for a pulse from Z_2 and from Z_{tr}. But the inductance as seen from the impedance producing the pulse is different for each PD source. For example a pulse coming from Z_2 sees a small inductance to Z_1 and Z_{tcce} and a larger inductance to Z_{tr}. While a pulse coming from Z_{tr} sees a small inductance to Z_{tcce} a larger inductance to Z_2 and an even larger inductance to Z_1. This is not the case when the circuit is modelled with only parallel impedances and inductances. In that case the inductances are always the same. When the inductances are placed in the wire at the top of the equivalent circuit (Z_{l1}, Z_{l2} and Z_{l3}), $H_{tcce,1,out}$ is not the same for Z_2 and Z_{tcce}.

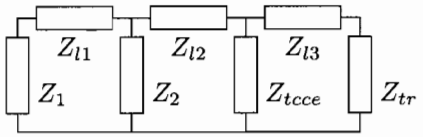

Figure 6.17: Alternative equivalent circuit

Chapter 7

Conclusions and recommendations

7.1 Inductive sensors

7.1.1 Transfer impedance

The transfer impedance of both developed coils is higher than the sensitivity criterium of 1 V/A for the major part of the frequency range of interest, namely from 2 – 3 MHz up to 30 MHz.

The desired frequency range is not accomplished. Above 10 MHz, the environment and the rest of the measurement system have an unknown influence on the transfer impedance. Because in a practical situation, the transfer impedance is unknown above approximately 10 MHz, it can not be used to accurately measure higher frequencies. The desired upper limit, 30 MHz, is not reached. This limit can be improved if the resonances can be damped. [And71] describes a method to damp resonances in Rogowski coils, by placing resistors between the turns. For the coaxial cable coil the resonance is already relatively small.

7.1.2 Electrical shielding effectiveness

With the developed electrical shielding test set-up the electrical shielding effectiveness of Rogowski coils can be determined. The shielding of the coaxial cable coil is about 2 – 3 times more effective the shielding of the copper wire coil. With the coaxial cable the coupling to the environment is worse, but the same injected current causes a smaller signal at the output. Overall the disturbing signal at the output of the coaxial cable coil is smaller. There are more options to shield a coil. E.g. a shield around the entire coil, a different configuration of the screen of the coaxial cable or another type of coaxial cable with better screening properties. A complete shielding, except for a slit of course, makes the coil less flexible for installing in RMUs.

7.2 Directional sensing

Two directional sensing techniques are proposed: Polarity-of-First-Peak (PFP) sensing and Directional and Differential sensing (DirecDiff) sensing.

7.2.1 Polarity-of-First-Peak technique

The PFP directional sensing technique works on the small test board as well as for the large KEMA test set-up. Both for far end injection and local injection the PFP sensing technique accurately determines the pulse direction. Also pulses from the transformer are correctly recognised as outgoing pulses. One drawback of this method is that the pulses must be clearly separated from each other. When an incoming and an outgoing pulse (from different sources) arrive at the same time, the resulting signal is seen as one signal and not as an incoming and an outgoing pulse. Another disadvantage of this technique is that it is more complicated to automate than the DirecDiff technique.

7.2.2 DirecDiff technique

The second directional sensing technique (DirecDiff sensing) can be applied as well. For the calibration of this method an incoming and an outgoing calibration pulse are required. When calibrated with pulses injected at the far end, pulses coming from the 10kV cables are filtered very well. If pulses injected locally are used to calibrate the sensing method the results are also usable, but somewhat less perfect as far end injection.

For the best results, far end injected pulses should be used for the calibration. Manually injecting pulses a the far end of both 10kV cables is time consuming in practice. A possible alternative is use PDs themselves for the calibration. This can only be achieved when clear distinguishable PD signals are obtained from both the cable under test and an outgoing cable. Further research is required to test this method for calibration.

The major drawback of the DirecDiff method however, no matter where the calibration pulses are injected, is that the pulses from the transformer are not recognised and filtered correctly. This makes the method unusable if also the transformer is a PD source. More research is required to find a way to correctly recognise and filter transformer PDs. One way to do this, is looking to the frequency content. PDs from nearby equipment still have high frequencies, which is obviously not the case for signals having travelled over a long cable.

Another way to cope with multiple disturbing PD sources, is to use two DirecDiff filters. One calibrated with an outgoing pulse from the cable *not* and the other calibrated with an outgoing pulse from the transformer. A recorded pulse is filtered with both filters. If the filtered signal of one of the filters is equal to zero, it is an outgoing pulse. If both filtered signals are not equal to zero, it is an incoming pulse.

Bibliography

[And71] Anderson, J.M.
Wide frequency range current transformer.
Review of Scientific Instruments, Vol. 42 (1971), No. 7, p. 915–926.

[Bau87] Baum, C.E. and E.L. Breen, J.C. Giles, J. O'Neill, G.D. Sower
Sensors for electromagnetic pulse measurements both inside and away from nuclear source regions.
IEEE Trans. on Antennas and Propagration, Vol. AP-26 (1978), No. 1, p. 22–35.

[Bel85] Bellm, H and A. Küchler, J. Herold, A. Schwab
Rogowski-spulen und Magnetfeldsensoren zur Messung transienter Ströme im Nanosecundenbereich (Teil 1 und Teil 2).
Archiv für Elektrotechnik, Vol. 68 (1985), p. 63–74.

[Bos00] Bossche, A. van den and J. Ghijselen
EMC Combined di/dt Current Probe.
IEEE Int. Symp. on Electromagnetic Compatebility, Washington, Aug. 21–25, 2000.

[Bur87] Burnley, K.G.
On-line monitoring of arcing and sparking phenomena in generators.
In Proc. 3rd Int. Conf. on Electrical Machines and Drivers, London, November 16-18, 1987.
London: IEE, 1987. P. 38–42.

[Cal91] Calico, S.E. and M.T. Crawford, M. Kristiansen, H. Krompholz
The design and calibration of a very fast current probe for short pulse measurements.
Review of Scientific Instruments, Vol. 62 (1991), No. 6, p. 1511–1513.

[Coo63] Cooper, J.
On the high frequency response of a Rogowski coil.
Plasma Physics (Journal of Nuclear Energy Part C), Vol. 5 (1963), p. 285–289.

[Ell80] Ellison, D.H. and J.L.T. Exon, D.A. Ward
Protection of slip-ring induction motors.
IEE 2nd Int. Conf. on Developments in Power System Protection, Savoy Place, June 10–12, 1980.
London: IEE, 1980. P. 49–53.

[Ger02] Gerasimov, A.I.
Wide-Range Inductive Sensors of Currents with Nanosecond Rise Times for Measuring Parameters of High-Current Pulses (Review).
Instruments and Experimental Techniques, Vol. 45 (2002), No. 2, p. 147–161.
Translated from: Pribory i Tekhnika Eksperimenta, No. 2 (2002), p. 5–20.

[Ham01] Hamerling, B.R. and F.J. Wester, E. Gulski, J.J. Smit, E.R.S. Groot
Fundamental aspects of on-line PD measurements on distribution power cables.
In: Proc. of the 2001 IEEE 7th Int. Conf. of Solid Dielectrics, Eindhoven, the Netherlands, June 25–29, 2001.
Piscataway: IEEE, 2001. P. 408–411.

[Hel95] Helvoort, M.J.A.M. van
Grounding structures for the EMC-protection of cabling and wiring.
Eindhoven (the Netherlands): Eindhoven University of Technology, 1995.
Doctoral dissertation.

[Hud65] Huddlestone, R.H. and S.L. Leonard
Plasma diagnostic techniques.
London: Academic Press, 1965.

[Nas79] Nassisi, V and A. Luches
Rogowski coils; theory and experimental results.
Review of Scientific Instruments, Vol. 50 (1979), No. 7, p. 900–902.

[Nev03] Nevalainen, P. and K. Nousaiainen
Rogowski Coil in Partial Discharge Measurements on MV Networks.
Nordic Insulation Symposium, Tampere, Finland, June 11–13, 2003.

[Oli54] Oliver, B.M.
Directional Electromagnetic Couplers.
Proc. of the Institute of Radio Engineers, Vol. 42 (1954), pp. 1686–1692.

[Pel71] Pellinen, D.G.
A Subnanosecond Risetime Fluxmeter.
Review of Scientific Instruments, Vol. 42 (1971), No. 5, p. 667–670.

[Pem00] Pemen, A.J.M.
Detection of partial discharges in stator windings of turbine generators.
Eindhoven (the Netherlands): Eindhoven University of Technology, 2000.
Doctoral dissertation.

[Pem93] Pemen, A.J.M. and P.C.T. van der Laan, P.T.M. Vaessen
Sensors for partial discharge monitoring of turbo generators.
Conf. Proc. 28th Universities Power Engineering Conf. (UPEC), Staffordshire, United Kingdom, September 1993.
Stafford: Staffordshire University, 1993. Vol. 2, p. 594–597.

[Pem95] Pemen, A.J.M. and P.T.M. Vaessen, P.C.T. van der Laan
On-line monitoring of statorwindings using partial discharge measurements.
Proc. of the 9th Int. Symp. on High Voltage Engineering, Graz, Aug 28 – Sep 1, 1995.
Graz: Inst. High Voltage Engineering, 1995. Vol. 5, paper 5059.

[Pet83] Pettinga, J.A.J. and J. Siersema
A polyphase 500 kA current measuring system with Rogowski coil.
IEE Proc. B Electric Power Applications, Vol. 130 (1983), No 5, p. 360–363.

[Pom99] Pommerenke, D and T. Strehl, R. Heinrich, W. Kalkner, F. Schmidt, W. Weißenberg
Discrimination between Internal PD and Other Pulses Using Directional Coupling Sensors on HV Cable Systems.
IEEE Trans. on Dielectrics and Electrical Insulation, Vol. 6, No. 6 (December 1999), pp. 814–824.

[Rog12] Rogowski, W. and W. Steinhaus
Die Messung der magnetischen Spannung.
Archiv für Elektrotechnik, Vol. 1 (1912), No. 4, pp. 141–150.

[Ste04] Steennis, E.F.
TU/e lecture Underground Power Cables
Chapter 10: Testing related to service operation
Eindhoven University of Technology, March 2004, pp. 10-7

[Sty82] Stygar, W. and G. Gerdin
High Frequency Rogowski Coil Response Characteristics.
IEEE Trans. on Plasma Science, Vol. PS-10 (1982), No. 1, p. 40–44.

[Vae04] Vaessen, G.A.J.
Ontwerpen van een Rogowski-spoel met coax-kabel.
Eindhoven University of Technoology, Department of Electrical Engineering, Electrical Power Systems Group, practical training report no. EPS.04.***.***

[War93] Ward, D.A. and J. La T. Exon
Using Rogowski coils for transient current measurements.
Engineering Science and Education Journal, Vol. 2 (1993), No. 3, pp. 105–113.

[Wen95] Wenzel, D and U. Schichler, H. Borsi, E. Gockenbach
Recognition of Partial Discharges on Power Units by Directional Coupling.
Proc. of the 9th Int. Symp. on High Voltage Engineering, Graz, Aug 28 – Sep 1, 1995.
Graz: Inst. High Voltage Engineering, 1995. paper 5626.

[Wie03] Wielen, P.C.J.M. van der and J. Veen, P.A.A.F. Wouters, E.F. Steennis
Sensors for On-line PD Detection in MV Power Cablea and their Locations in Substations.
7th Int. Conf. on Properties and Applications of Dielectric Materials, Nagoya, Japan, June 1–5, 2003.

[Won90] Wong, K.L. and T.R. Chen
Studies of a Slow-Wave Rogowski Coil.
IEEE Trans. on Plasma Science, Vol. 18 (1990), No. 2, p. 219–222.

[Won91] Wong, K.L.
New Structure For a Slow-Wave Rogowski Coil.
IEEE Trans. on Plasma Science, Vol. 19 (1991), No. 6, p. 1290–1991.

[Zon00] Zondervan, J.P. and E. Gulski, J.J. Smit
Fundamental aspects of PD patterns of on-line measurements on turbogenerators.
IEEE Trans. on Dielectrics and Electrical Insulation, Vol. 7 (2000), No. 1, p. 59–70.

[Zon98] Zondervan, J.P. and E. Gulski, J.J. Smit, R. Brooks
Use of the VHF detection technique for PD pattern analysis on turbogenerators.
Conf. Record of the 1998 IEEE Int. Symp. on Electrical Insulation, Arlington, USA, June 7–10, 1998.
New York: IEEE, 1998. Vol. 1, p. 274–277.

[Zon99] Zondervan, J.P. and E. Gulski, J.J. Smit, T. Grun, M. Turner
A new multi-purpose partial discharge analyser for on-site and on-line diagnosis of high voltage components.
11th Int. Symp. on High Voltage Engineering, Conf. Publ. No. 467, London, August 22–27, 1999.
London: IEE, 1999. Vol. 5, p. 348–351.

Appendix A

Nomenclature RMU

In an RMU there are several locations where a current sensor can be clamped around a conductor to measure the current. A schematic drawing with the relevant parts of the RMU is depicted in figure A.1. The names for the sensor locations and the currents at the different locations are listed in table A.1. Table A.2 lists the abbreviations used in the names for the sensor locations in the RMU.

Name	**Current symbol**	**SP impedance were current measured at this point flows through**
10kV PLEC	i_{plec}	Z_{plec} in case one cable
If more than one cable: 10kV PLEC 1 10kV PLEC 2	If more than one cable: $i_{1,plec}$, $i_{2,plec}$ (counted from TCC) or shorter: i_1, i_2 (if there is no need to make a difference between i_{plec} and i_{lec})	If more cables: $Z_{1,plec}$, $Z_{2,plec}$ (1 = next to TCC) or shorter: Z_1, Z_2
Last earth connection 10kV If more than one cable: Earth 10kV 1 Earth 10kV 2	i_{lec} If more than one cable: $i_{1,lec}$, $i_{2,lec}$ (counted from TCC)	↑ same as 10kV PLEC ↑
3 TCC	i_{3tcc}	Z_{3tcc}
Earth TCC	i_{tcce}	Z_{tcce}
TCC yellow, blue or red	$i_{tcc,y}$, $i_{tcc,b}$ or $i_{tcc,r}$	-
Transformer	i_{tr}	Z_{tr}

Table A.1: Name and symbols for the positions in an RMU

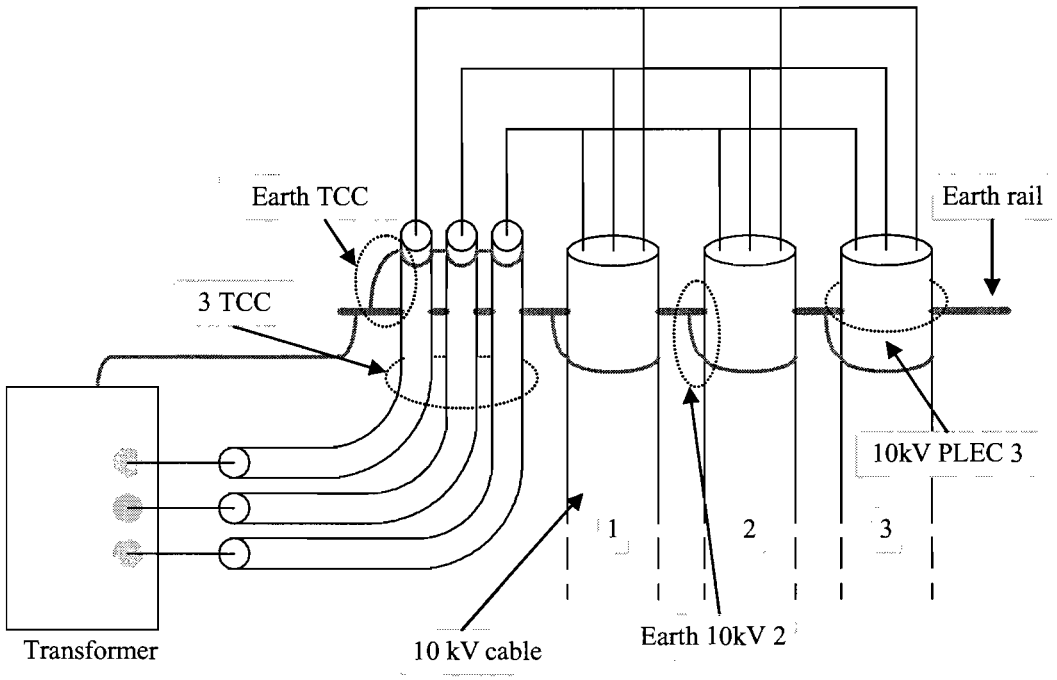

Figure A.1: Schematic drawing of an RMU

Name	Abbreviation
Past Last Earth Connection	PLEC
Phase-to-Phase	PP
Shield-to-Phase	SP
Transformer Connecting Cable(s)	TCC

Table A.2: Abbreviations used in position names

Appendix B

Literature research

In this appendix the literature research report is printed that made for the course Practical Library Training. In this report a major part of the literature research done for the graduation project is described in detail.

Summary M.Sc. project

The M.Sc. project is part of a larger research project. The goal of that project is to develop a system to measure partial discharges (PD) in medium voltage power system cables. The partial discharge measurement has to take place on-line, without interrupting the power delivery. The M.Sc. project concerns the sensors for this system. Below are the goals for the M.Sc. project.

1. Research and design Rogowski coils for on-line partial discharge detection in medium voltage power system cables. Optimise the sensors (dimensions, number of windings, integrators, etc ...) for different sensor locations, propagation channels.
2. Research the need for and different options to shield these sensors
3. Calibration of the developed sensors
4. Make the sensors directional by using the correct combinations of measuring locations and transformation and interpretation of the measured signals.
5. Search for easy to use materials for the core of the Rogowski coil.

Literature research goals

During the literature research only literature for item number 1 of the M.Sc. project summary (see section above) is searched for. The literature research goals are:

- Search for information about inductive current sensors used for monitoring partial discharges (PD's). Not necessarily for monitoring PD's in cables, sensors to monitor currents in transformers, generators, cable joints, etc... are relevant too. It has to be possible to

install the sensors while the monitored object is in service. The sensor has to be usable under noisy conditions.

- The literature should provide information on the fundamental principles, a description of the sensors properties and/or design considerations.
- The publication type is irrelevant. The fundamental principles of the Rogowski coil will most probably be explained in books since the principles were already published in 1912.
- The Rogowski coil has been used for decades for several purposes. In the last few decades the Rogowski coil has used to monitor partial discharge in devices. Therefore the research period is set from 1960 to present. It is not necessary to find very recent literature about the subject because the sensor has been used and studied for decades.
- The literature research is not limited to country or research facility.

A practical trainee has done a literature research about the Rogowski coil in general. Therefore this literature research focuses on inductive sensors especially for PD monitoring.

Concept table of contents of graduation report

1. Summary
2. Introduction
3. Rogowski coil theory
4. Shielding
5. Design
6. Calibration
7. Experiments
8. Directional sensor
9. Conclusions

Search terms

The search terms below were used to search for literature. Two or more of these terms were used together in several combinations.

- Partial discharge*
- PD*

- Rogowski
- Sensor*
- Inductive
- On-line or online or on line
- Cable*
- Measurement or measure or measuring
- Monitoring or monitor

In Vubis the Dutch translations of these search terms have been used also.

Consulted sources

The table lists the consulted sources. The sources were consulted in the order they are in the table. The last column lists the number of new references that were initially selected using that source. If a reference was selected earlier in another database, the reference is not added again to the "No. of selected items" column. The initial selection of the references was made based on title and abstract (if available).

Source	Consulted via	Searched period	No. of selected items
TU/e catalogus	Vubis	all	7
IEEE-IEE Electronic Library	IEEE Xplore	1960–present	19
INSPEC	WebSPIRS	1969–present	5
Compendex	ScienceDirect	1966–present	0
ETDE Energy Database	ETDEWEB	1974–present	0
Google	www.google.nl	all	1

Selection criteria

Since most sources provide an abstract together with the title, both were used to make the first selection. For the sources where no abstract was available, the first selection was made based on just the title. If the title and abstract contain the following information the publication is selected. When there was doubt on the usability of the publication the reference was selected.

+ Information about the theory and design of inductive sensors for on-line partial discharge measurement.
+ Because PD's have a wide bandwidth, references about high frequency Rogowski coils are selected.
+ The reference contains information about shielding inductive PD sensors from a noisy (lots of disturbing EM fields) environment. Or sensors used in a noisy environment.

+ The reference is about a complete on-line PD measurement system for on-line PD monitoring. Because the sensors are part of the complete system, it is likely that the reference will contain a description of the sensor or references to other literature describing the sensors.

Publications were rejected because of the following reasons:

- If only other types of sensors were used for PD detection the publication is not selected.
- The sensor is only usable to detect PD's in cables with a helical earth screen.
- In the past several off-line PD measurement systems have been developed. A description of an off-line PD measurement system is not selected because those systems don't use inductive sensors.
- References in other languages than Dutch, English or German are rejected. The reference is kept for possibly later usage.

For the final selection the full text is retrieved. The full text is judged on the same criteria as for the initial selection. All publications are read and judged whether they contain useful information. If they do, the publication is selected. If not, the publication still might have references to useful publications. The location of the reference in the full text often gives excellent information about the contents of that reference. If a publication itself does not contain useful information, but it has good references, the publication is selected anyway. This is done to be able to complete the snowball method diagram. To distinguish these publications from publications with information on the M.Sc. subject, these publications are printed in *italic* in the references list in section 11 and in the snowball diagram.

In several cases the reference does not contain information useful for the M.Sc. project and has no direct references to useful publications. Often these publications do contain references to other publications about on-line PD measurement. Because these new publications might have references to useful information, they are selected anyway. The newly found references are retrieved and judged in the same way. This process is repeated until no more good references are found. If in the end the entire thread does not contain any useful information or references to useful information the entire thread is rejected afterwards. As above here also the publications not containing useful information themselves are printed in *italic* in the references list and on the snowball method diagram.

Snowball method

- The snowball search was started with [PEM00]. This is a recent doctoral dissertation with a chapter describing the design of a Rogowski coil used for on-line PD monitoring in a generator. In this chapter the developed sensor is described in detail. The references in the text of the chapter seem to point to some good publications.
- A second starting point is [NEV03]. This is a recent publication that describes a Rogowski coil developed for on-line PD measurement. This coil is used in a situation similar to the situation of the M.Sc. project.

- A third starting point is [WIE03]. A publication of the same project as the M.Sc. project. Therefore it deals with sensors for the exact same application. Also the publication is of a very recent date.

In figure B.1 on page 62 the snowball diagram is shown.

Citation method

Sources

The table lists the sources consulted for the citation method. The sources were consulted in the order they are in the table. The last column lists the number of new references that were selected using that source. If a reference was selected earlier in another database or with another search method the reference is not added again to the "No. of selected items" column.

Source	Consulted via	Searched period	No. of selected items
Science Citation Index Expanded	Web of Science	all (1988–2004)	4
IEEE-IEE Electronic Library	IEEE Xplore	1960–2004	0
Compendex	ScienceDirect	all (1994–2004)	0

Starting publications

Because the snowball method revealed several relatively old publications there are several options for starting publications. A practical trainee already has done literature research on the Rogowksi coil in general. A few publications found with the snowball searching method were found earlier by the practical trainee. Because he already performed the citation method on these publications, they were not used again as a starting publication. All other publications were used as a starting publication for the citation search method.

The citation diagram is plotted in figure B.2 on page 63.

Relations pattern

Chapter	'12	'60–'69	'70–'79	'80–'89	'90–'99	'00–'04
1. Introduction	[Rog12]					[Nev03]
2. Rogowski coil theory	[Rog12]		[Bau78] [Nas79] [Pel71]	[Bel85] [Bur87] [Pet83] [Sty82]	[War93] [Won90]	[Pem00] [Wie03]
3. Shielding			[Bau78]	[Bel85]	[Hel95] [Won90]	[Ger02]
4. Design			[Bau78]	[Pet83]	[Cal91] [Hel95] [Won03]	[Ger02] [Nev03] [Pem00]
5. Calibration			[Nas79] [Pel71]	[Ell80]	[Cal91]	[Nev03]
6. Experiments	[Rog12]		[Nas79] [Pel71]	[Bel85] [Ell80]	[Pem93] [Won03]	[Nev03] [Pem00]
7. Directional sensor						
8. Conclusions						[Nev03]

Conclusions

The found literature can be roughly divided into two categories:. The first category focuses on the measurements and analysis of partial discharges. Virtually all publications in this category describe the used sensors only briefly or not at all. The second category focuses on the sensor itself. In most cases this sensor is not developed specifically for the measurement of partial discharges. But the theory and a lot of the design considerations are the same for different sensor applications.

The literature research shows that the Rogowski coil can be used in different ways. By changing the properties of the coil, the materials used and the connected impedance the response of the Rogowski coil can be changed. The coil is highly insensitive to external noise sources and this insensitivity can be even more improved with a complete shield or the use of a coaxial cable. Inductive current sensors have been used to measure partial discharges under noisy conditions.

The most cited publication is the original publication that describes the Rogowski coil by W. Rogowski and W. Steinhaus [Rog12]. An important company researching the off line and on line measurement of partial discharges is KEMA in Arnhem. On the Rogowski coil in general, the publication by D.A. Ward [War93] is cited a lot. This is a very informative article about the Rogowski coil, theory and different applications. Another publication cited a lot is [Coo63] by J. Cooper. This is a publication relatively old, but still cited a lot. It seems to be the first publication describing the Rogowski coil with earth screen as a delay line.

A practical trainee conducted literature research earlier on the Rogowski coil in general. The practical trainee found only four publications found in this literature study [Nev03], [Pet83],

[Rog12] and [War93]. This shows that is was useful to conduct the literature research on almost the same subject, but with a different approach. One of the publications was about the same research project as the M.Sc. project [Wie03], it was written by the supervisors. The rest of the publications were new.

Diagrams

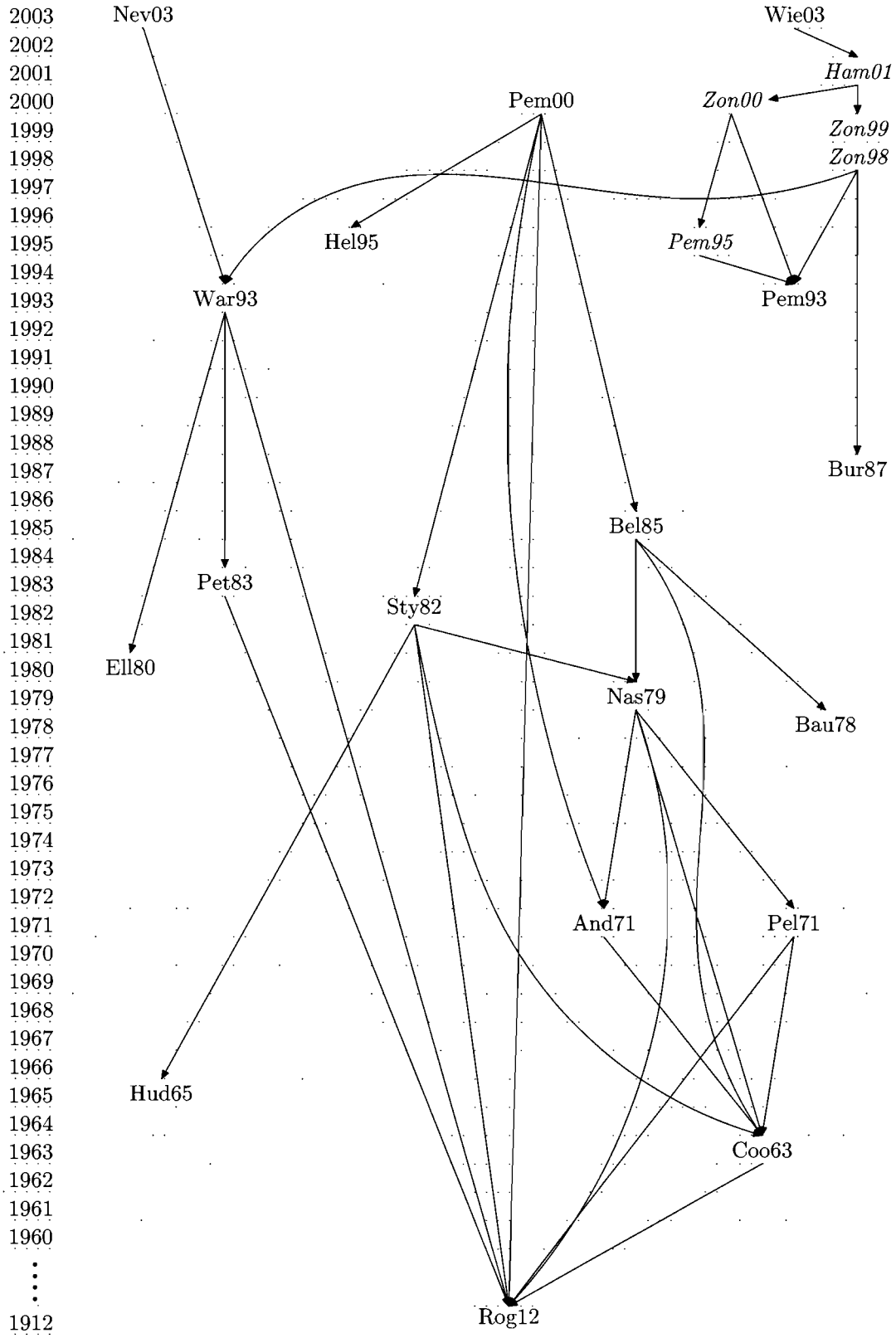

Figure B.1: Snowball diagram

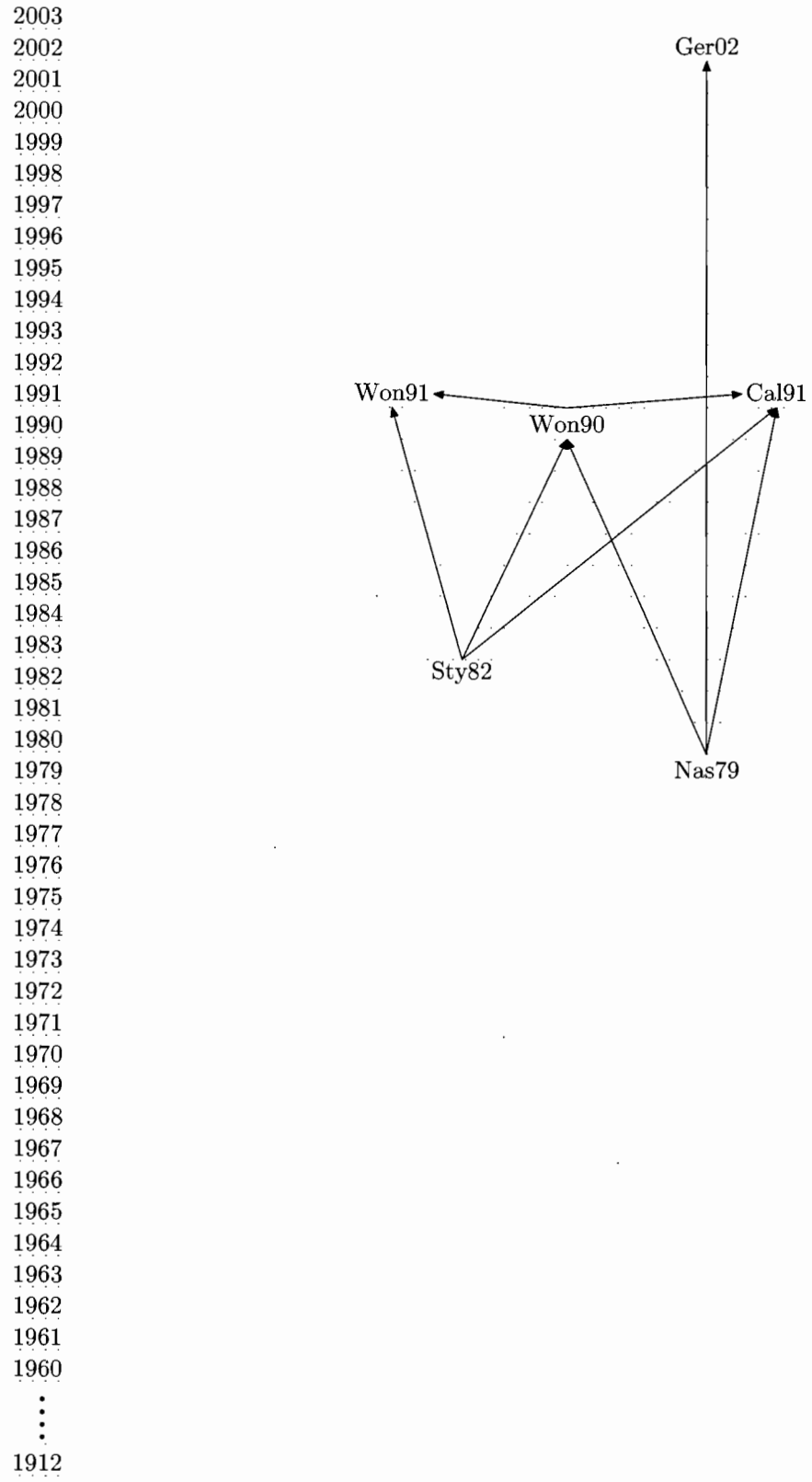

Figure B.2: Citation diagram